Computers & Industrial Engineering 162 (2021) 107647

Contents lists available at ScienceDirect

Computers & Industrial Engineering

journal homepage: www.elsevier.com/locate/caie

Supply curves of electricity-based gaseous fuels in the MENA region

Benjamin Lux [a,*], Johanna Gegenheimer [b], Katja Franke [a], Frank Sensfuß [a], Benjamin Pfluger [c]

[a] Fraunhofer Institute for Systems and Innovation Research ISI, Breslauer Straße 48, 76139 Karlsruhe, Germany
[b] DVGW Research Center at Engler-Bunte-Institut of Karlsruhe Institute of Technology (KIT), Engler-Bunte-Ring 1-9, Building 40.51, 76131 Karlsruhe, Germany
[c] Fraunhofer Research Institution for Energy Infrastructures and Geothermal Systems IEG, Breslauer Straße 48, 76139 Karlsruhe, Germany

ARTICLE INFO

Keywords:
E-Fuels
Power-to-Gas
MENA region
Energy system modeling
Cost of hydrogen
Cost of synthetic methane

ABSTRACT

The utilization of electricity-based fuels (e-fuels) is a potential strategy component for achieving greenhouse gas neutrality in the European Union (EU). As renewable electricity production sites in the EU itself might be scarce and relatively expensive, importing e-fuels from the Middle East and North Africa (MENA) could be a complementary and cost-efficient option. Using the energy system model Enertile, supply curves for hydrogen and synthetic methane in the MENA region are determined for the years 2030 and 2050 to evaluate this import option techno-economically. The model optimizes investments in renewable electricity production, e-fuel production chains, and local electricity transport infrastructures. Analyses of renewable electricity generation potentials show that the MENA region in particular has large low-cost solar power potentials. Optimization results in Enertile show for a weighted average cost of capital of 7% that substantial hydrogen production starts above 100 €/MWh_{H2} in 2030 and above 70 €/MWh_{H2} in 2050. Substantial synthetic methane production in the model results starts above 170 €/MWh_{CH4} in 2030 and above 120 €/MWh_{CH4} in 2050. The most important cost component in both fuel production routes is electricity. Taking into account transport cost surcharges, in Europe synthetic methane from MENA is available above 180 €/MWh_{CH4} in 2030 and above 130 €/MWh_{CH4} in 2050. Hydrogen exports from MENA to Europe cost above 120 €/MWh_{H2} in 2030 and above 90 €/MWh_{H2} in 2050. If exported to Europe, both e-fuels are more expensive to produce and transport in liquefied form than in gaseous form. A comparison of European hydrogen supply curves with hydrogen imports from MENA for 2050 reveals that imports can only be economically efficient if the two following conditions are met: Firstly, similar interest rates prevail in the EU and MENA; secondly, hydrogen transport costs converge at the cheap end of the range in the current literature. Apart from this, a shortage of land for renewable electricity generation in Europe may lead to hydrogen imports from MENA. This analysis is intended to assist in guiding European industrial and energy policy, planning import infrastructure needs, and providing an analytical framework for project developers in the MENA region.

1. Introduction

To counter the threats of global warming, the international community of states agreed in the 2015 Paris Agreement to balance greenhouse gas (GHG) emissions and sinks in the second half of the 21st century (United Nations, 2015). Subsequently, the European Commission (EC) sharpened their climate protection target in the European Green Deal and is now aiming for GHG neutrality by 2050 (Council of the European Union, 2009; European Commission, 2019). While all scenarios in the EC's underlying in-depth analysis (European Commission, 2018a, 2018b) make strong use of energy efficiency measures and renewable energy sources (RES), the scenarios with net-zero GHG emissions in 2050 also strongly rely on electricity-based hydrogen (H_2) and other synthetic fuels. In its "Hydrogen Strategy" the EC makes hydrogen a key priority to achieve Europe's clean energy transition (European Commission, 2020). Overall, these electricity-based fuels (e-fuels[1]) are climate-neutral substitutes for fossil fuels, assuming that only renewable electricity and balance-neutral carbon sources are used in the synthesis process (Graves, Ebbesen, Mogensen, & Lackner, 2011; Zeman & Keith, 2008). Substituting fossil fuels with e-

* Corresponding author.
E-mail addresses: benjamin.lux@isi.fraunhofer.de (B. Lux), gegenheimer@dvgw-ebi.de (J. Gegenheimer), katja.franke@isi.fraunhofer.de (K. Franke), frank.sensfuss@isi.fraunhofer.de (F. Sensfuß), benjamin.pfluger@ieg.fraunhofer.de (B. Pfluger).

[1] "E-fuels" is the umbrella term for all gaseous energy carriers produced from electricity considered in this article.

https://doi.org/10.1016/j.cie.2021.107647

Available online 28 August 2021

fuels offers the advantage of reducing carbon dioxide (CO_2) emissions across sectors while continuing to use well-established application technologies. For gaseous and liquid hydrocarbons, most existing infrastructures can be retained.

The deployment of e-fuels is heavily dependent on costs and available quantities. These two properties in turn depend on the availability of suitable RES. If e-fuels are to play a substantial role, large additional amounts of renewable electricity are required. In Europe itself, the availability of land for renewable electricity generation to produce e-fuels may be limited due to high electricity demands and low acceptance of renewable generation facilities. Therefore, importing e-fuels might be an alternative, complementary, or even necessary option. In addition, the production of e-fuels in regions close to the equator could be more cost-efficient due to favorable solar conditions. However, other cost factors such as transportation to Europe or the availability of climate-neutral CO_2 for fuel synthesis must be taken into account. For Europe, the MENA (Middle East and North Africa) region is of particular interest as a potential exporter of e-fuels.

Few peer-reviewed studies have examined in detail the generation potential of e-fuels in the MENA region, their generation costs, and their potential export to Europe:

Timmerberg and Kaltschmitt (2019) investigate the cost and potentials of electricity-based hydrogen in North Africa and its transport to Europe as a blend with natural gas in existing pipelines. Hydrogen production is therefore investigated only in the vicinity of existing natural gas pipelines in North Africa. Using linear optimization, hydrogen supply costs from MENA to Central Europe in 2020 amount to between 54 €/MWh_{H2} and 119 €/MWh_{H2} depending on the underlying parameter scenario. Timmerberg and Kaltschmitt (2019) find that the existing pipeline capacity is the limiting factor and not the potentials of renewable energies required for hydrogen supply from North Africa to Central Europe.

Hank et al. (2020a) develop five Power-to-X (PtX) pathways (methane, methanol, ammonia, liquefied hydrogen, and hydrogen bound in liquid organic hydrogen carriers). In a case study, they evaluate these PtX pathways for an exemplary medium- to large-scale production site in Morocco for the year 2030. The analysis is based solely on local renewable electricity generation. Downstream long-distance transport to Northwestern Europe is part of the cost assessment. Gaseous hydrogen in Morocco has an ex works production cost of 90 €/$MWh_{H2,LHV}$[2]. Additional liquefaction, intermediate storage, and shipping from Morocco to Germany increases the hydrogen supply cost to 126 €/$MWh_{H2,LHV}$. Gaseous synthetic methane (CH_4) is available in Morocco at a production cost of 124 €/$MWh_{CH4,LHV}$. Liquefied transport to Germany increases the methane supply cost to 145 €/$MWh_{CH4,LHV}$.

Ueckerdt et al. (2021) estimate the supply cost of synthetic methane produced in a renewable-rich country and subsequently shipped for about 4,000 km. The basis of their analysis is an average electricity price of 50 €/MWh_{el} in 2030 and 30 €/MWh_{el} in 2050, which reflects the average costs of electricity supply of a wind- and solar PV-based power system in Australia. They determine cost-optimal electrolysis utilization using the electricity price variability of wholesale market data for Australia as of 2019. They assume that their analysis could fit the supply of e-fuels produced in Northwest Africa (e.g. Morocco) and transported to Northwest Europe (e.g. Germany). For 2030 they estimate a synthetic methane supply cost of 114 €/$MWh_{CH4,LHV}$[3] in Europe. For 2050 their estimate is 65 €/$MWh_{CH4,LHV}$[3].

In addition to peer-reviewed literature, there is also grey literature and online tools that address e-fuels generation in the MENA region. The International Energy Agency (2019) identifies North Africa and the Middle East as promising areas for electricity-based hydrogen production. It estimates the cost of electrolytic hydrogen in the long-term as 43 €/$MWh_{H2,LHV}$ in the Middle East[3 and 4] and 41 €/$MW_{H2,LHV}$ in North Africa[3 and 4]. Agora Verkehrswende, Agora Energiewende, and Frontier Economics (2018) estimate the final product cost of synthetic methane in North Africa and the Middle East as 140 €/MWh_{CH4} in 2030 and to 110 €/MWh_{CH4} in 2050. They base their cost estimates on PV and hybrid PV-wind power systems. Fraunhofer IEE (2021) has developed a PtX potential atlas in a web application. The atlas shows the generation potential for hydrogen and various synthetic hydrocarbons in 2050 for selected locations worldwide. It also provides information on transport costs from the PtX production site to Europe. As an example, production and liquefaction of hydrogen at a production site in Morocco and subsequent transport to Germany costs on average 102 €/MWh_{H2} in 2050. The export of liquefied synthetic methane costs 127 €/MWh_{CH4} for the same country combination.

There is currently no literature that looks in detail at e-fuel generation in the MENA region beyond individual site assessments. Based on these preliminary considerations the central research questions in this paper are:

- What is the techno-economic generation potential of the e-fuels hydrogen and synthetic methane in the MENA region?
- What is the optimal power generation mix for e-fuel production in MENA?
- Which countries offer the most favorable conditions for the production of hydrogen and synthetic methane?
- Which technical components of e-fuel production are decisive for the generation costs?
- How does e-fuel generation in MENA perform compared to Europe, and are exports to Europe feasible?

Addressing these questions will make it possible to derive strategies for future European e-fuel imports, for example by allowing domestic production options in Europe to be weighed against imports. Since the lead time for infrastructures such as gas pipelines is typically several years, an assessment of whether there is a need for transportation infrastructure from the MENA region to Europe is valuable. Additionally, the derived costs are valuable for determining use cases of e-fuels in various sectors and for comparing strategies based on e-fuel against other decarbonization options.

The analysis of the generation potentials of electricity-based hydrogen and synthetic methane in the MENA region is conducted for the years 2030 and 2050 using an energy system optimization model. The approach requires that e-fuel production is based solely on renewable electricity.

The paper is structured as follows: Section 2 introduces the modelling approach, scenario design, and most important input parameters including e-fuel production chains. Section 3 presents the model results. Section 4 summarizes the findings and derives key conclusions.

2. Methodology and data

2.1. Methodology

E-fuel supply curves in the MENA region are calculated and analyzed using the energy system model *Enertile* (Fraunhofer Institute for Systems and Innovation Research [ISI], 2019). *Enertile* is a software package aimed at optimizing the future cost of energy supply in Europe and the MENA region. It combines the interlinked supply of electricity, heat, and

[2] The energy content of hydrogen is given in terms of the lower heating value (LHV) of hydrogen, which describes the amount of thermal energy released during the combustion of hydrogen without water condensation.

[3] Values read from a figure.

[4] Values in International Energy Agency (2019) are given in USD/kg_{H2}. Conversion with energy content of hydrogen related to the lower heating value 33.33 kWh_{H2}/kg_{H2} and the average USD-EURO exchange rate in 2019 of 1 Euro = 1.12 USD.

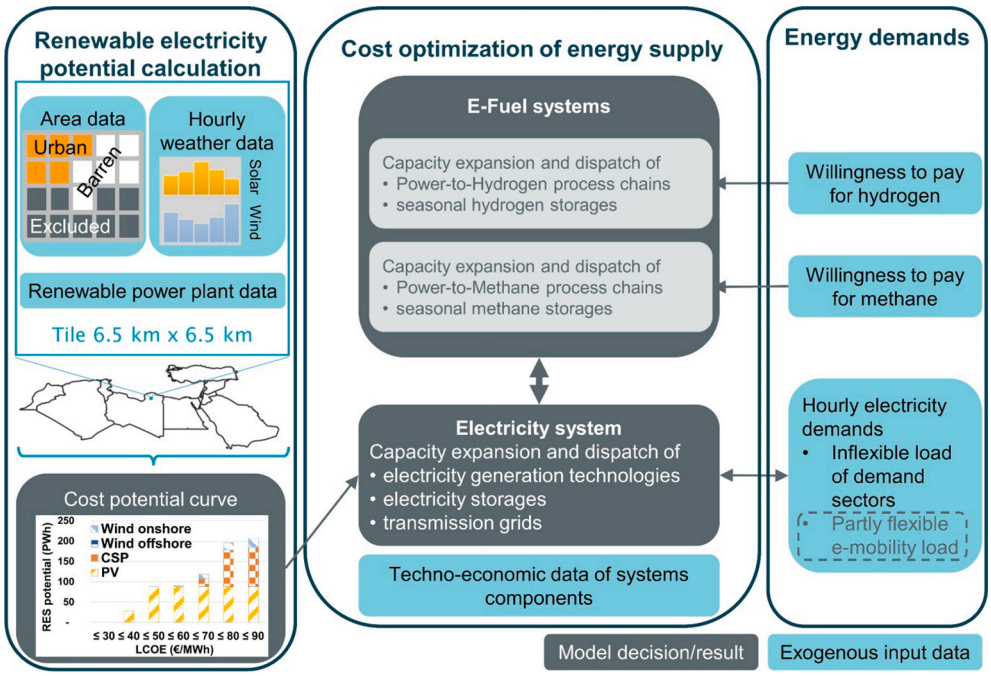

Fig. 1. Simplified graphical illustration of the components and interactions of the energy system model *Enertile* as used in this paper. Calculations for Europe, which serve as a benchmark for the results of this paper, additionally cover heat generation in heat grids (cf. Lux and Pfluger (2020)).

electricity-based fuels with highly resolved potentials of solar and wind energy.

2.1.1. *Energy system model Enertile*

Enertile is an optimization model with a high technical, spatial, and temporal resolution. It determines the cost-minimal portfolio of technologies to meet exogenously specified electricity, heat, and e-fuel demands simultaneously. However, calculations in the MENA region use only the electricity and e-fuel supply modules. Fig. 1 shows a simplified illustration of the model components used in this paper. The optimization includes both capacity expansion and unit dispatch of relevant generation and infrastructure technologies. The portfolio of technologies covers renewable energies, in particular wind and solar energy, conventional power plants, electricity transmission grids, e-fuel generation technologies, energy storage facilities, and demand-side flexibility options. A more detailed and formal description of *Enertile* and how it is used to determine hydrogen supply curves can be found in Lux and Pfluger (2020). Pfluger (2014) describes the model representation of the electricity system more thoroughly, though for an older version not including e-fuels; Bernath, Deac, and Sensfuß (2019) provide a detailed insight into the heat module of *Enertile* that is used for calculations in Europe. The central extension of *Enertile* in this paper provides a model representation of process chains for the generation of synthetic methane and a regional concept of the MENA region for e-fuel production. The methodology for determining synthetic methane supply curves follows the computational procedure for hydrogen supply curves outlined in Lux and Pfluger (2020). Subsequent paragraphs summarize the key properties of the optimization model for the analysis in this paper.

The objective function of the optimization model totals the cost of the supply side of the energy system being considered, including electricity transport and storage. Installed capacities of energy infrastructures and their hourly dispatch are the decision variables of the linear problem. These variables are weighted by fixed costs and variable costs in the objective function. Fixed costs for expanding the capacity of a specific technology include annuitized investments and fixed operation and maintenance costs. Utilizing the technology incurs variable costs, including fuel costs, CO_2 emission costs and variable costs for operation and maintenance.

The central constraints of the optimization problem require hourly equilibria of energy supply and demand in balance equations. These balance equations are formulated for electricity and electricity-based fuels for each model region and each hour of a given year. Demands either are given exogenously or arise endogenously as a model decision. An endogenous electricity demand arises, for example, from the model-determined use of electrolyzers. Sector coupling options, energy storages, and grids create connections between individual balancing equations. Sector coupling technologies such as electrolyzers enter the electricity and hydrogen balance of a given region and hour with either a plus or minus sign as appropriate. Storages create intertemporal connections between balancing equations. Electricity transmission grids link electricity balances in different regions. This allows *Enertile* to provide a very detailed picture of the interdependencies of the energy supply side in the optimization process. Other constraints ensure that system components operate within their capacity limits.

The provision of e-fuels plays a special role in the modeling for this paper. In contrast to exogenous electricity demands, there are no e-fuel demands externally imposed on *Enertile*. Instead, the model is offered a selling price for hydrogen or synthetic methane and it decides how much e-fuel it will produce at the given price. Technically, the sale of e-fuels reduces the energy system cost in the objective function. The model installs and uses additional electricity supply infrastructure and e-fuel generation units as long as incurred costs are covered by the revenues of selling these e-fuels. The last megawatt-hour of e-fuels provided and sold creates marginal costs at almost exactly the applied sales price. This mechanism can represent potential e-fuel demands from other sectors in the MENA region or export offers at the relevant sales price. Applying different sales prices in different model runs generates cost-supply curves for the investigated e-fuels. These supply curves interrelate with the rest of the energy system in the scenario design. It is also possible to use e-fuels exclusively for energy storage within the model.

The linear optimization problem is set up and solved for the simulation years 2030 and 2050 in hourly resolution. The expansion and dispatch of energy infrastructures are optimized using perfect foresight. The full hourly resolution of analyzed years combined with the use of real weather data allows an adequate representation of the challenging synchronization between energy demand and fluctuating renewable

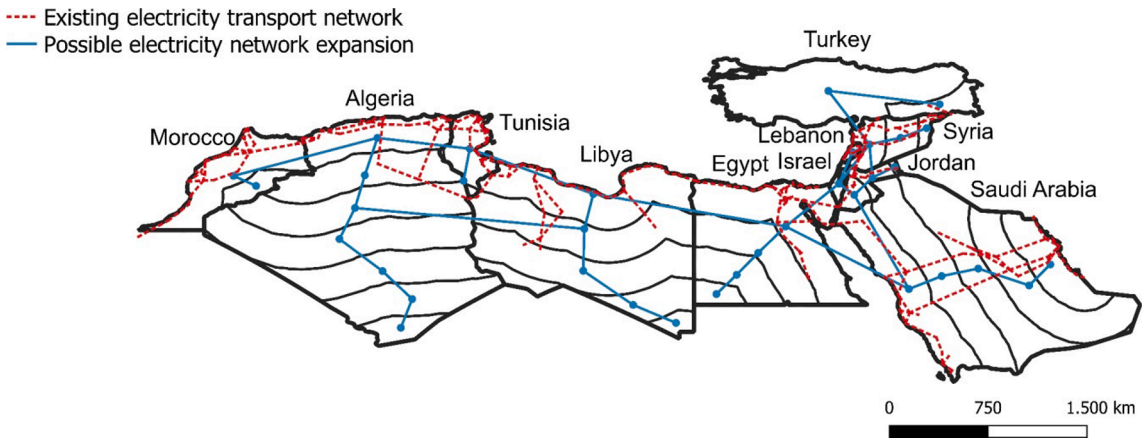

Fig. 2. Geographic coverage of the modeling approach, existing electricity transport network (Beltaifa, 2020), and modelled net transfer capacities as electricity grid between regions.

Table 1
Utilization factors for the considered land uses and renewable technologies.

Land use	Onshore wind (ID 166 & 168)	Offshore wind (ID 104 & 117)	Ground-mounted PV (ID 133 & 140)	Rooftop PV (ID 97 & 102)	CSP (ID 89 & 94)
Barren	0.4	0	0.16	0	0.12
Cropland natural	0	0	0	0	0
Croplands	0.3	0	0	0	0.01
Forest	0.15	0	0	0	0
Grassland	0.3	0	0.2	0	0.02
Savanna	0.3	0	0.2	0	0.12
Scrubland	0.3	0	0.2	0	0.12
Snow and ice	0.12	0	0.4	0	0
Urban	0	0	0	0.065	0
Water	0	0.9	0	0	0
Wetlands	0	0	0	0	0
Excluded	0	0	0	0	0

Own assumptions.

energy supply. This approach can allow for extreme weather events from the energy system perspective with simultaneous lulls, cold spells, and darkness.

For the analysis in this paper, *Enertile* covers the energy supply system in Morocco, Algeria, Libya, Tunisia, Egypt, Saudi Arabia, Lebanon, Israel, Syria, and Turkey. While renewable potentials are determined on a regionally highly resolved grid with a size of 42.25 km^2, electricity demands and trade flows are summarized in larger model regions. Due to the extensive geographical area of the countries under consideration, the concentration of population and infrastructures near the coasts, and the generally high aridity of the area, model regions are defined as a function of distance to coast. Fig. 2 shows that the analyzed countries are divided into 250 km wide strips starting at the coast. Model regions with coastline access and therefore seawater access have a special status, as in the selected modeling approach e-fuels can only be produced here. This means that electrolyzers and subsequent synthesis plants can only be built near the coast and operated with desalinated seawater. This approach is intended to prevent competition for scarce fresh water in the arid MENA region and water transport across the desert.

The electricity transport grid in *Enertile* is modeled as net transfer capacities (NTCs) between different model regions. Fig. 2 shows the potential grid connections. The modeling of electricity transport grids for the MENA region follows three approaches. Firstly, it enables the expansion of the power grid between model regions already connected through transmission lines. Fig. 2 shows the existing transmission network connections based on a dataset of Beltaifa (2020). Secondly, grid expansion becomes possible between coastal regions of neighboring countries, regardless of whether connections already exist or not. Thirdly, grid connections between coastal regions and the hinterland can be created or extended. The last two approaches allow for the power supply of e-fuel generation units near the coast and ensure that the entire MENA region can contribute to e-fuel production. Local grid restrictions within model regions are not considered and unlimited flows are allowed within the model regions.

2.1.2. Renewable potential calculation

The calculation of the potentials of renewable energies is an upstream process to *Enertile* (cf. Fig. 1). Geographically resolved power generation potentials are determined on the basis of real weather data, land use data, and techno-economic parameters of renewable power generation technologies. The analysis includes onshore wind, offshore wind, ground-mounted photovoltaics (PV), and concentrated solar power (CSP) technologies. As a result, *Enertile* obtains installable capacities, full load hours of power generation, hourly generation profiles, and levelized costs of electricity for the energy system optimization.

Following the definition of different potential types for renewable energies in Hoogwijk, Vries, and Turkenburg (2004), the geographical potential, the technical potential, and the economic potential are each determined in turn. The basis of all these potential calculations is the division of the MENA region into a grid with an edge length of 6.5 × 6.5 km. More than 250,000 tiles are evaluated for the entire region under consideration.

The first step is to determine the geographical potential, expressing the area assessable for the installation of renewable energies for each tile of the grid. For this analysis, each grid tile receives information on land use (European Space Agency and Université Catholique de Louvain, 2010), elevation and slope (Danielson & Gesch, 2011), and protected areas (World Conservation Monitoring Centre [UNEP], 2014). Tiles located in protected areas or near cities are excluded from the calculation. The approach considers geo-technical limitations such as excessive slopes (e.g. for CSP) or high water depth (e.g. for offshore wind). For each land use type and renewable technology, a utilization factor is defined that determines the proportion allowed for renewable electricity generation. Table 1 lists the utilization factors for different land uses and technologies. The available area per tile for a renewable technology is calculated using equation (1). In (1) A_{tile} is the area of each tile (42.25 km^2), $share_l$ is the share of the land use type l on this tile, and u_l is the utilization factor for this land use and technology. The sum of the available area of the 250,000 tiles results in the geographical potential A_{region} of the model region.

$$A_{region} = \sum^{tile} A_{tile} \bullet share_l \bullet u_l \quad (1)$$

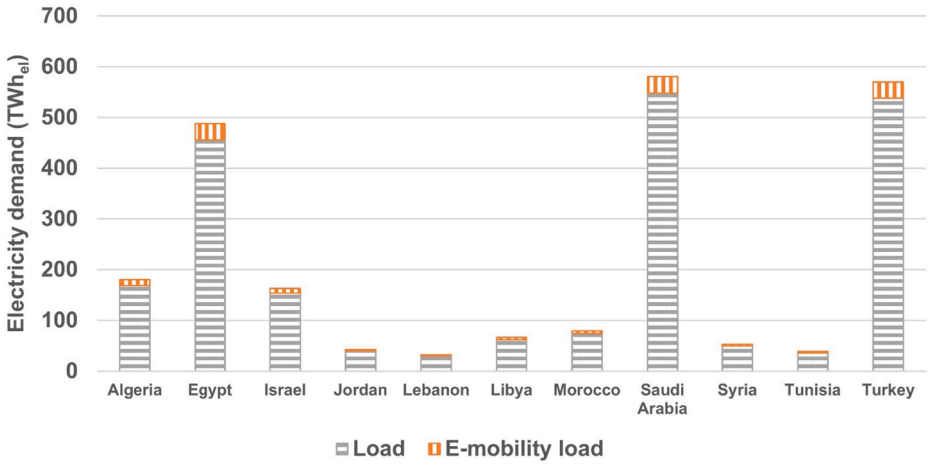

Fig. 3. Projected electricity demands in the MENA countries in 2050. Electricity demands include a flat surcharge for distribution grid losses of 6.5%.

Renewable power generation potentials are sensitive to assumptions on utilization factors for different land uses and renewable technologies. Throughout the literature, utilization factors vary widely. Franke, Sensfuß, Deac, Kleinschmitt, and Ragwitz (2021) analyze the dependency of onshore wind potentials on the chosen utilization factors. This study shows that land utilization factors can have an impact of up to 51% on the calculated results. The utilization factors used in this paper tend to be lower than the values in most literature. As *Enertile* can build different renewable technologies on a single tile, competition for available space can arise for certain technologies and land use categories. The chosen utilization factors are intended to reflect this competition. In reviewed publications (Bosch, Staffell, & Hawkes, 2017; Eurek et al., 2017; Feng, Feng, Wang, & King, 2020; He & Kammen, 2014; Hu, Harmsen, Crijns-Graus, & Worrell, 2019; Liu, Wang, & Zhu, 2017; Sebestyén, 2017), the utilization factors vary between 0.0 and 0.9 for the land use category "barren". In the MENA region, this category accounts for a high share of up to 80% in Egypt, Libya, and Algeria. The chosen utilization factor for this land use therefore has a huge impact on the calculated potentials. In this study, the chosen utilization factor is low to represent a conservative approach. The actual potential of renewable energies could therefore be higher.

In the second step, the technical potential of renewable energies is determined. The technical potential describes the maximum installable capacity of renewable energy technologies per tile. This is achieved by intersecting the available areas determined in the geographical potential with the technical limitations of the power generation technologies. In the case of wind power, the spacing of the turbines in the field is taken into account to limit the wind shadow effect. The spacing used in this article is 5 rotor diameters within a row and 9 rotor diameters between rows (Gupta, 2016; Pfluger et al., 2017). The occupied area of solar power plants is dependent on the efficiency of the solar power plant. The installable capacity of solar power plants varies from 50 MW/km^2 for a module with an efficiency of 17% to 57 MW/km^2 for a module with an efficiency of 19% (Fraunhofer ISE, 2015). This installable capacity is based upon an analysis of the occupied area by real solar power plants. Different azimuth and tilt angles are also considered (Schubert, 2012).

Finally, the economic potentials are determined. The economic potential comprises the levelized cost of electricity per tile and technology. In this step, the technical potential is combined with techno-economic data of renewable power generation technologies and real weather data for a selected weather year. The technology-specific cost data include both specific investments for capacity expansion and the costs of operation and maintenance. For wind power, the installation costs are dependent on the hub height and rotor diameter. In the calculated scenarios, the model can choose between 59 different turbine configurations for onshore wind and seven offshore wind turbines (cf. Appendix A.5). For onshore wind, the number of different wind turbine configurations increases from 10 in 2020 to 30 in 2030 and 41 in 2040. In the case of wind turbines, the future cost reduction potential of individual components such as rotors, generators, or towers is limited due to the already high level of technological maturity. Electricity generation from wind could become cheaper in the future if larger plants are built, the rotor-generator ratio increases and the plant can specifically absorb more energy. In this paper, it is assumed that the specific investments show a cost reduction of about 10% between 2020 and 2050. For example, a wind turbine with a hub height of 110 m and a specific area output of 400 W$_{el}$/m^2 costs 1160 €/kW$_{el}$ in 2020 and 1050 €/kW$_{el}$ in 2050. For PV plants, modules are currently still learning at a rate of 19% (Zentrum für Sonnenenergie- und Wasserstoff-Forschung Baden-Württemberg, 2019). There is still potential for cost reductions and efficiency improvements. As module prices fall, other components, such as the rack, become increasingly important. However, the technical learning of these peripheral systems and thus the cost reduction potential is limited and thus slows down the technical learning of the entire system. Reductions in specific investments and operation and maintenance costs are taken into account for each renewable power generation technology considered, as shown in the appendix in Tables A7 and A8.

The specific electricity production costs also depend on the assumed full load hours and related electricity generation of the technologies. In this modeling, the operating times are derived from real weather data for the year 2010. For wind power plants, the wind speed at four different heights is considered to calculate the electricity output. For solar plants, the solar irradiation and the temperature are taken into account. Further information on the calculated power output can be found in Schubert (2012). The data base for hourly wind speed, solar irradiation, and temperature is the ERA5 dataset from the European Centre for Medium-Range Weather Forecasts (Copernicus Climate Change Service, 2020).

2.2. Data

2.2.1. General framework and scenario design

This article examines the supply of electricity-based hydrogen and synthetic methane in the MENA region in the years 2030 and 2050. A fundamental premise is that the electricity used in e-fuel generation originates from RES. To guarantee this renewable origin, the optimization framework differs for the two target years.

According to the politically set expansion targets for renewable energies, the electricity mix of the MENA countries will still be dominated by fossil energies in 2030 (Timmerberg, Sanna, Kaltschmitt, & Finkbeiner, 2019). Morocco sets the most ambitious target, with renewables accounting for an envisaged 52% of its national electricity production in

Table 2
Techno-economic characteristics of the transmission grid parametrization in *Enertile* (Godron et al., 2014).

Technology	CAPEX	Fixed OPEX	Losses
Converter terminal	270 M€	1% of investment p.a.	3% per 1000 km [(a)]
High-voltage direct current (HVDC) overhead line	300 €/(MW_{el} km)	1% of investment p.a.	

a) Own estimations

2030 (Timmerberg et al., 2019). A greenfield approach for e-fuel production is therefore assumed with respect to the power system in 2030. The optimizer's expandable technology portfolio is limited to renewable energies, electricity storages, and grid infrastructure. In the optimization problem, the remaining electricity demand of the MENA states and the existing power plant fleet and transport infrastructure are excluded. This ensures the additivity of the renewable power generation units and power infrastructures to be installed for e-fuel production, as they are operated completely independently from the rest of the electricity system, which is not modeled. Consequently, a synergetic utilization of electricity infrastructures to meet electricity demands in MENA and to generate hydrogen or synthetic methane is not possible in this setting.

For 2050, it is assumed that all electricity generation in MENA is greenhouse gas neutral. Fossil generation technologies are prohibited in the modeling approach. The optimization problem addresses the cost-efficient supply of electricity demands in MENA and the supply of electricity-based fuels. Mutual synergies can be exploited.

Demands or exports of hydrogen or synthetic methane are not explicitly modeled. Instead, the model has the option of reducing system costs by generating and selling these e-fuels. No distinction is made between sales to demand sectors in MENA and exports, as the sales price is interpreted as the price ex works. In a parameter study, the associated hydrogen and methane sales prices are increased in steps of 10 €/$MWh_{H2/CH4,LHV}$.

2.2.2. Electricity demands in the MENA region in 2050

Electricity demands for each MENA country in 2050 are estimated using historical demands from 2018 (IEA, 2020), average annual load growth rates from the World Energy Outlook 2020 (International Energy Agency, 2020), and population projections from the United Nations in 2019 (United Nations, Department of Economic and Social Affairs, Population Division, 2019). Fig. 3 shows the resulting load projections for the MENA region in 2050. The identified electricity demands are distributed among the different model regions within a country according to the population distribution from 2018 (WorldPop, 2018). The modeling distinguishes between electricity demands that follow a fixed demand profile and those that have some flexibility. The general load in Fig. 3 follows a fixed demand profile. Electricity demands for e-mobility have an inflexible and a flexible component. The inflexible mobility demand includes trolley trucks, trolley buses, and battery electric vehicles with inflexible charging behavior. For 50% of battery electric vehicles, it is assumed that they can charge flexibly while complying with their driving profiles.

2.2.3. Electricity transport network expansion

The parameterization of the NTCs of the modeled power grid is based on the data in Table 2. Specific investments and losses of grid lines are weighted by the distances between geographic centers of connected model regions in the transport network parameterization in *Enertile*.

2.2.4. E-fuel production concepts

This section presents the conceptual design of e-fuel production chains in the MENA region. It illustrates eight different generation concepts for electricity-based hydrogen and methane and their techno-economic parametrization in the energy system model *Enertile*.

The efficient conversion of electricity into hydrogen and methane, called the Power-to-Gas (PtG) process, requires the interaction of different technologies. Depending on the final product, these technologies include seawater desalination, water electrolysis, CO_2 supply, methanation and liquefaction units. *Enertile* takes the energy system perspective and is thus unable to resolve these individual components.

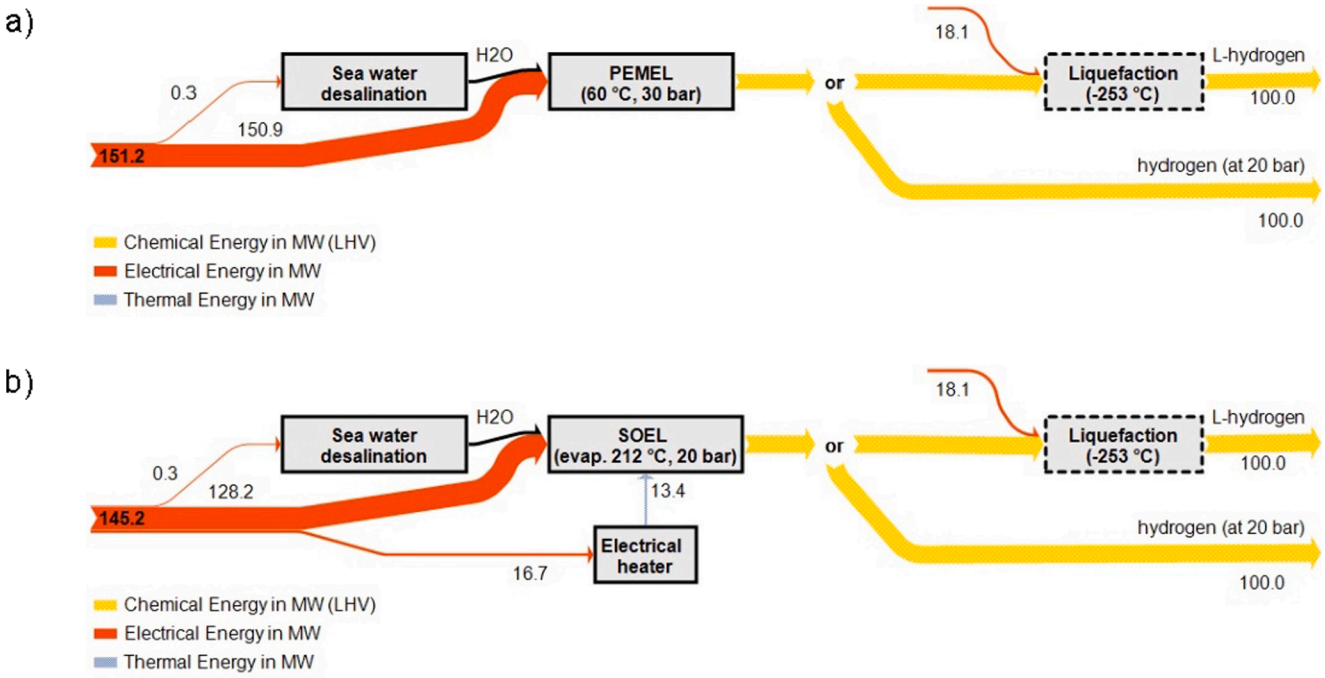

Fig. 4. Energy flow diagram for a Power-to-Hydrogen process chain in the MENA region with PEMEL (a) or SOEL (b) and optional liquefaction for 100 MW hydrogen output related to the lower heating value (LHV). The process chains are based on technical key data referring to the year 2050. Quantities of energy not shown correspond to energetic losses.

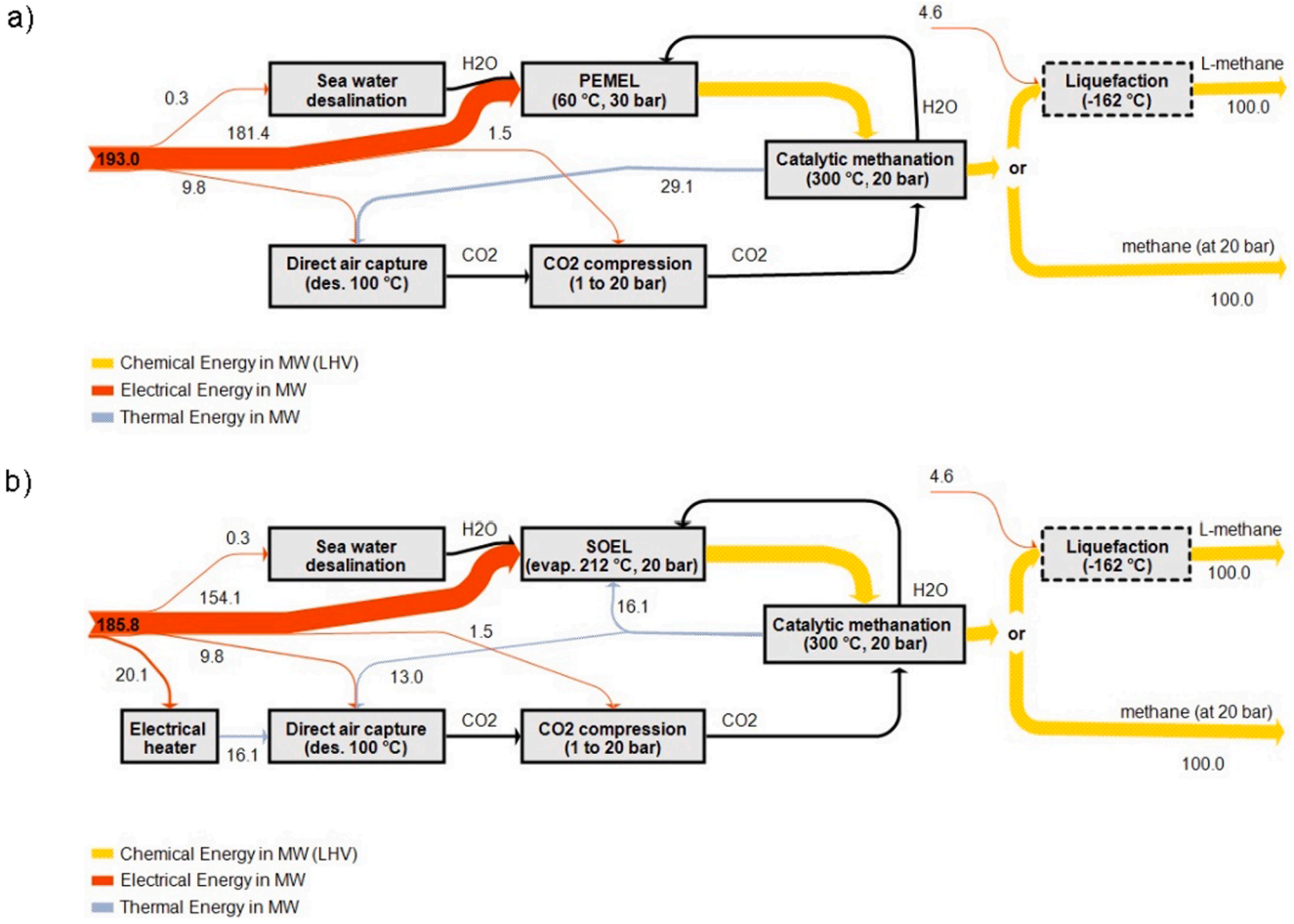

Fig. 5. Energy flow diagram for a Power-to-Methane process chain in the MENA region with PEMEL (a) or SOEL (b) and optional liquefaction for 100 MW methane output related to the lower heating value (LHV). The process chains are based on technical key data referring to the year 2050. Quantities of energy not shown correspond to energetic losses.

Table 3
Overall efficiencies of the four investigated options of Power-to-Hydrogen (PtH_2) process chains in MENA, based on technical key data referring to the years 2030 and 2050. Values are related to the lower heating value (LHV) and take internal heat integration into account. External heat requirements are provided by an electric heater.

Power-to-Hydrogen production chain	Overall efficiency $\eta_{PtCH4,LHV}$ in %	
	in 2030	in 2050
PtH_2-PEMEL	60	66
PtH_2-SOEL	68	69
PtH_2-PEMEL-liquefaction	53	59
PtH_2-SOEL-liquefaction	60	61

Therefore, a preliminary analysis assembles four representative production chains for hydrogen (Power-to-Hydrogen, PtH_2) and methane (Power-to-Methane, $PtCH_4$), respectively. These production chains enter the *Enertile* parametrization as an integrated composition characterized by overall efficiencies, summed specific investments, and aggregated operation and maintenance costs. The individual technologies in the production chains and their techno-economic characteristics as described in detail in appendix.

Hydrogen and methane production chains are differentiated in two aspects: the electrolyzer technology and the physical state of the final product. The physical state of the product can be either gaseous or liquefied. This paper distinguishes between e-fuel production chains with polymer electrolyte membrane electrolysis (PEMEL) and solid oxide electrolysis (SOEL). The analysis of all investigated process chains refers to technical and economic data for the year 2030 or 2050 and for a plant capacity of 100 $MW_{H2/CH4}$. In this article, the plant capacity or plant output ($MWh_{H2/CH4}$) are related to the lower heating value (LHV) of the product (i.e. hydrogen or methane), which describes the amount of thermal energy released during the product's combustion without water condensation. Fig. 4 and Fig. 5 show the considered production chains for gaseous hydrogen (at 20 bar) and liquefied hydrogen (L-hydrogen, L-H2) and for methane (L-methane, L-CH4) for the year 2050. Direct input parameters for the *Enertile* model are the overall process efficiencies and the specific costs of the entire process chains shown below. The energy balance of the production chains comprises chemical, electrical, and thermal energy inflows and outflows. Except for methanation, all processes within the investigated production chains have relevant electrical energy demands. SOEL and DAC have additional thermal energy demands. Due to the exothermic reaction, methanation releases thermal energy, which covers parts of the thermal energy demands of DAC and SOEL. An electric heater covers the remaining thermal energy requirements.

The overall process efficiency $\eta_{PtH2,LHV}$ or $\eta_{PtCH4,LHV}$ of e-fuel production in equations (2) and (3) is defined as the ratio of the chemical energy output $F_{E,chem,H2/CH4,LHV}$ in the form of hydrogen or methane to the electrical energy input $F_{E,el,total,in}$. The chemical energy output is defined as the product of the mass flow $F_{M,H2/CH4}$ and lower heating value of hydrogen or methane $LHV_{H2/CH4}$.

Table 4
Overall efficiencies of the four investigated options of Power-to-Methane ($PtCH_4$) process chains in MENA, based on technical key data referring to the years 2030 and 2050. Values are related to the lower heating value (LHV) and take internal heat integration into account. External heat requirements are provided by an electric heater.

Power-to-Methane production chain	Overall efficiency $\eta_{PtCH4,LHV}$ in %	
	in 2030	in 2050
$PtCH_4$-PEMEL	47	52
$PtCH_4$-SOEL	53	54
$PtCH_4$-PEMEL-liquefaction	46	51
$PtCH_4$-SOEL-liquefaction	52	53

$$\eta_{PtH2,LHV} = \frac{F_{E,chem,H2,LHV}}{F_{E,el,total,in}} = \frac{F_{M,H2} * LHV_{H2}}{F_{E,el,total,in}} \quad (2)$$

$$\eta_{PtCH4,LHV} = \frac{F_{E,chem,CH4,LHV}}{F_{E,el,total,in}} = \frac{F_{M,CH4} * LHV_{CH4}}{F_{E,el,total,in}} \quad (3)$$

Table 3 and Table 4 show the overall process efficiencies for the eight investigated PtH_2 and $PtCH_4$ process chains. These efficiencies match well with the literature and real-life data from pilot plants (Drechsler & Agar, 2021; Frank, Gorre, Ruoss, & Friedl, 2018; Götz et al., 2016; Timmerberg & Kaltschmitt, 2019). Theoretical optimization of the STORE&GO pilot plant in Troia, Italy, with a plant size of approximately 200 kW_{el} electrical input, shows that an overall PtG efficiency of 46 % related to the higher heating value (HHV) of the methane output is achievable, without taking into account further energy savings through scaling effects (Schlautmann et al., 2021).

Table 5 and Table 6 show specific capital expenditure (CAPEX) and fixed operating expenditure (OPEX) of the different PtH2 and PtCH4 production chains as used in *Enertile*. Costs to meet electricity demands are determined endogenously by the optimization model.

Today's PtG plants operate on a pilot scale of a few $MW_{H2/CH4}$. Due to the high RES generation potential in MENA, PtG plants on a gigawatt scale are likely in the future. The economic analyses in this article are examples based on key data for a plant capacity of 100 $MW_{H2/CH4,LHV}$ output. For plants with capacities of several hundred $MW_{H2/CH4}$, the costs may be lower due to degression. However, the CAPEX-intensive PtG technologies, such as electrolysis and DAC, are modular and larger plant capacities are achieved by numbering up. Whether the assumed cost reductions for the PtG technologies will be achieved in 2030 and 2050 depends largely on the actual market ramp-up of PtG. For this reason, the learning rates predicted in the literature may be either under- or over-fulfilled.

Table 7
Levelized transport costs for hydrogen and synthetic methane referring to the lower heating value (LHV) of hydrogen or methane. Costs for transport via ship exclude liquefaction. Costs for transport via pipeline include on-site compression up to 100 bar for hydrogen and up to 80 bar for methane. Costs are based on values for 2020 and rely on a literature review (Fasold, 2010; Homann et al., 2013; IEA, 2019; Leiblein et al., 2020; Göß, 2017).

Logistic chain	Levelized costs of transport	
Hydrogen via pipeline	0.69	€ct/(MWh_{H2} km)
Hydrogen via ship	$12.43 \times x^{0.13}$, x : *distance in km*	€/MWh_{H2}
Synthetic methane via pipeline	0.17	€ct/(MWh_{CH4} km)
Synthetic methane via ship	$0.11 \times x^{0.38}$, x : *distance in km*	€/MWh_{CH4}

2.2.5. Long-distance transport of e-fuels

Hydrogen and methane have low energy densities compared to fossil liquid fuels such as petroleum. To transport these fuels economically, they must be compressed or liquefied. Alternatively, hydrogen can be converted to larger molecules, which is not considered in this article.

The logistic concept for pipeline-based transport of hydrogen and synthetic methane essentially includes compressor stations, transport pipelines, and gas storage facilities. The long-distance transport of liquefied hydrogen or methane consists of the sub-steps of liquefaction and intermediate storage, transport via tankers, and regasification on arrival.

Table 5
CAPEX and fixed OPEX for entire Power-to-Hydrogen (PtH_2) process chains in the MENA region. Underlying economic key data refer to the years 2030 and 2050 and to a plant capacity of 100 MW hydrogen or methane output related to the lower heating value (LHV) as listed in the appendix (Table A 5 and Table A 6).

Power-to-Hydrogen production chain		Specific costs		
		in 2030	in 2050	
PtH_2-PEMEL	CAPEX	689	623	€/kW_{H2}
	fixed OPEX	26	23	€/kW_{H2}/ a
PtH_2-SOEL	CAPEX	1,026	690	€/kW_{H2}
	fixed OPEX	77	37	€/kW_{H2}/ a
PtH_2-PEMEL-Liqufaction	CAPEX	1,756	1,690	€/kW_{H2}
	fixed OPEX	69	65	€/kW_{H2}/ a
PtH_2-SOEL-Liqufaction	CAPEX	2,061	1,757	€/kW_{H2}
	fixed OPEX	120	80	€/kW_{H2}/ a

Table 6
CAPEX and fixed OPEX for entire Power-to-Methane ($PtCH_4$) process chains in the MENA region. Underlying economic key data refer to the years 2030 and 2050 and to a plant capacity of 100 MW hydrogen or methane output related to the lower heating value (LHV) as listed in the appendix (Table A 5 and Table A 6).

Power-to-Methane production chain		Specific costs		
		in 2030	in 2050	
$PtCH_4$-PEMEL	CAPEX	1,968	1,516	€/kW_{CH4}
	fixed OPEX	58	45	€/kW_{CH4}/ a
$PtCH_4$-SOEL	CAPEX	2,373	1,595	€/kW_{CH44}
	fixed OPEX	120	63	€/kW_{CH4}/ a
$PtCH_4$-PEMEL-Liqufaction	CAPEX	2,493	2,038	€/kW_{CH4}
	fixed OPEX	90	77	€/kW_{CH4}/ a
$PtCH_4$-SOEL-Liqufaction	CAPEX	2,897	2,119	€/kW_{CH4}
	fixed OPEX	151	94	€/kW_{CH4}/ a

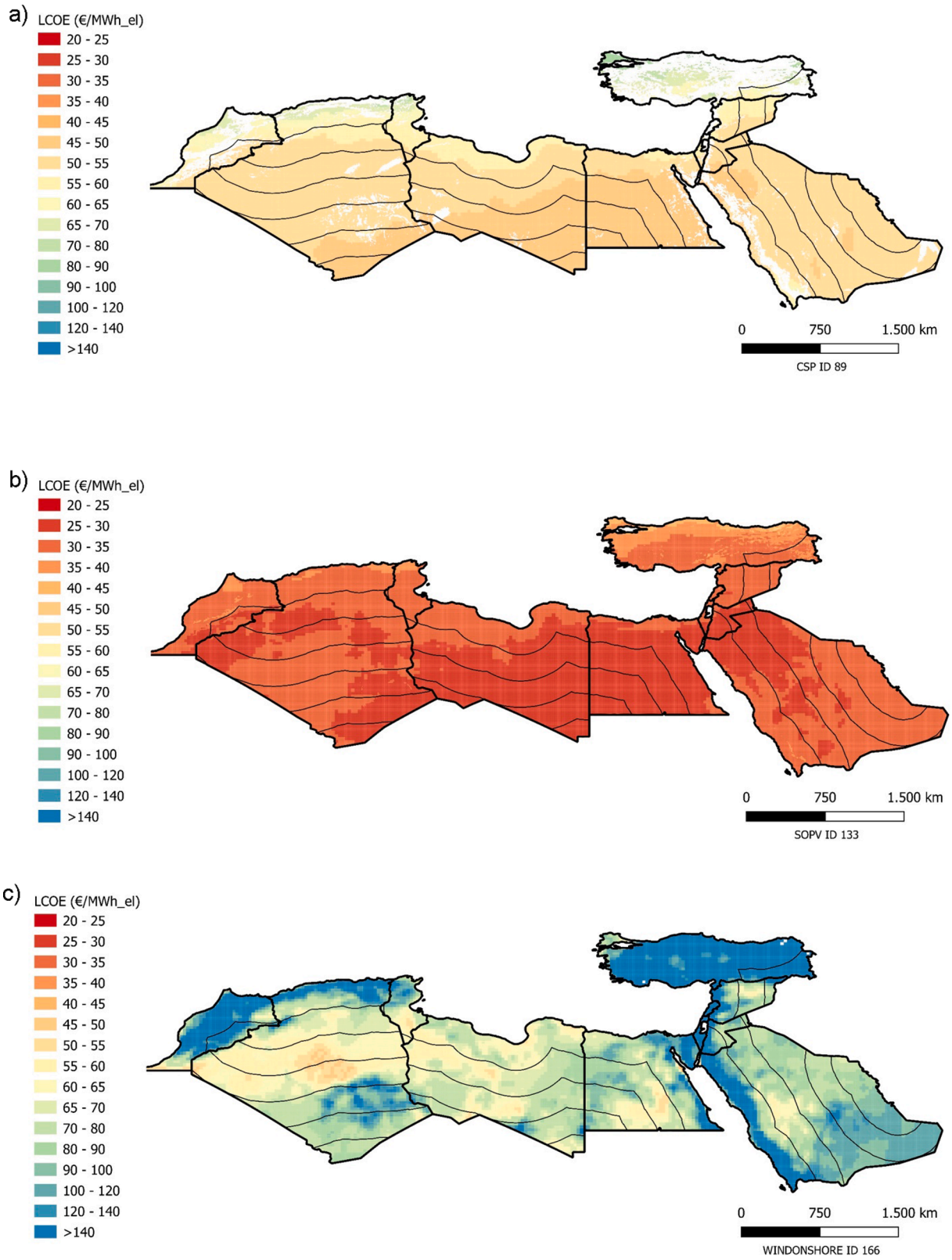

Fig. 6. Spatial distribution of LCOE for the technologies a) CSP, b) ground mounted PV, and c) onshore wind in 2050 calculated with a WACC of 7%. White spaces are excluded from the potential calculation due to excessive slopes.

The transport costs depend in particular on the distance to be covered. In this article, transport distances are estimated by the center-to-center air distance to e-fuel production regions in the MENA region (cf. section 2.1.1 and appendix) and continental Europe. In reality, transport routes are likely to be different.

For large methane volumes, pipeline transport is profitable for shorter distances, while transport of L-methane becomes economically feasible for larger distances (between 2,000 and 5,000 km). Liquid transportation is dominated by liquefaction costs, while pipeline-based transport requires more compressors as the distance increases

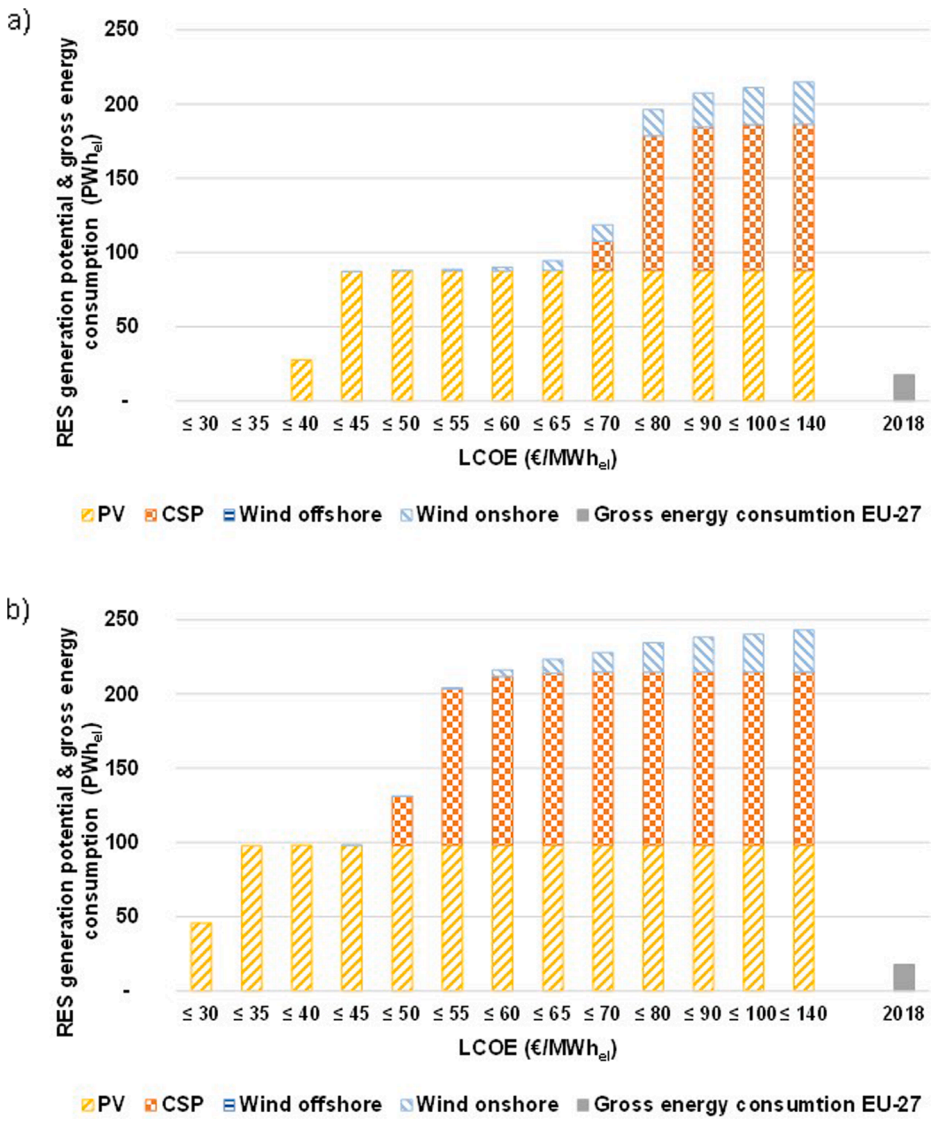

Fig. 7. Renewable potential curves for the various technologies in the MENA region for the years 2030 (a) and 2050 (b).

(Fasold, 2010; Homann, Reimert, & Klocke, 2013; Göß, 2017). The costs reported in the literature for transporting natural gas via pipelines and via ship vary mainly due to the different assumed capacities and distances. (Fasold, 2010; Homann et al., 2013; Deymann, 2014; Göß, 2017).

Today, hydrogen pipelines are mostly operated locally, e.g. at industrial sites, and a hydrogen tanker is operated only for project purposes (Collins, 2019). Due to limited experience, cost values for hydrogen transport vary widely in the literature (Hydrogen Council, 2020; IEA, 2019; Niermann, Timmerberg, Drünert, & Kaltschmitt, 2021). One of the main challenges is the low boiling temperature of hydrogen, compared to methane (see A.4). The shipping of hydrogen therefore shows higher costs, e.g. for the insulation of the tanks.

The compression of hydrogen is also more energy-intensive than of methane and thus, higher costs are expected for hydrogen pipelines. The transport costs of gaseous hydrogen strongly depend on the assumed pipeline capacities. Wang, van der Leun, Peters, and Buseman (2020) calculate costs for new infrastructure, assuming hydrogen pipelines with a diameter of 0.6 to 1.2 m and a nominal capacity of approximately 13 GW_{H2}. The author's own estimations (Leiblein et al., 2020) agree with the costs given by Wang et al. (2020). Table 7 shows the distance-dependent costs for the transport of hydrogen and synthetic methane from MENA to continental Europe used in this article.

3. Results

3.1. Renewable energy potentials in MENA

The supply of e-fuels decisively depends on the quantity and levelized cost of renewable electricity. This section therefore presents both the spatial distribution of the generation costs of the main renewable power generation technologies of PV, CSP, and onshore wind, and cumulative cost potential curves for renewable electricity for the MENA region.

3.1.1. Spatial distribution of renewable energies

Fig. 6 shows the spatial distribution of levelized cost of electricity (LCOE) for the generation technologies CSP (a), ground-mounted PV (b), and onshore wind (c) in the MENA region in 2050. The results in this figure are based on calculations with a weighted average cost of capital (WACC) of 7%.

Offshore wind is not considered in the following analysis, as the potentials are low in the MENA region. This is firstly due to the restriction that offshore wind can only be installed up to a water depth of 50 m and up to 370 km from the coast. In the Mediterranean Sea adjacent to the MENA region the water depth is mostly greater, so the installable capacities for offshore wind plants are low. Secondly, the full

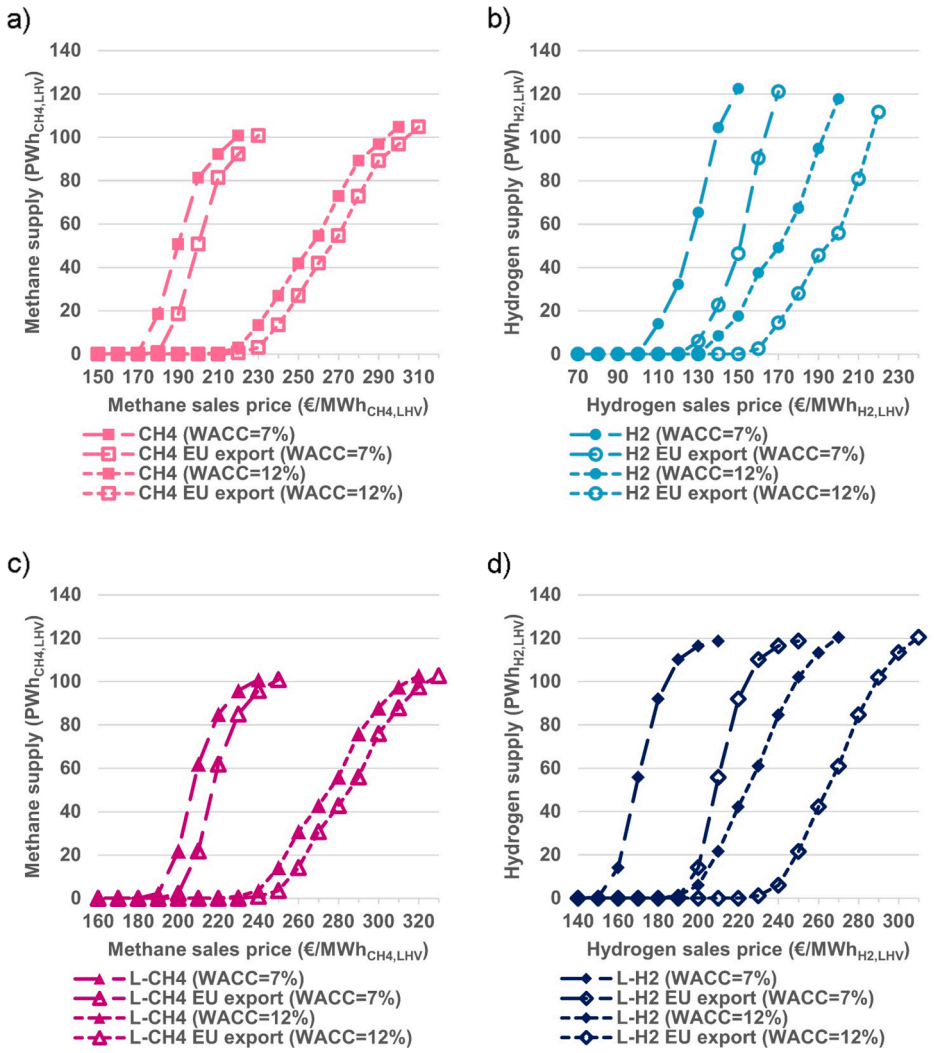

Fig. 8. Supply curves of e-fuels in the MENA region including and excluding transportation to the EU in 2030. Production and export quantities of a) methane (CH4), b) hydrogen (H2), c) liquefied methane (L-CH4), and d) liquefied hydrogen (L-H2) are shown for a weighted average cost of capital (WACC) of 7% and 12%.

load hours for offshore wind in the regions considered are mainly below 3,000 h. Overall, the electricity generation of offshore wind starts at a LCOE of 130 €/MWh$_{el}$.

Due to low installation costs, solar PV is the least expensive power generation technology in MENA in 2050, with a LCOE between 28 €/MWh$_{el}$ and 51 €/MWh$_{el}$. The uniform coloring of the map shows that the regional differences in LCOE are small. About 90% of the PV generation potential has electricity generation costs below 31 €/MWh$_{el}$. The overall cheapest 10% of the PV potential is located in Egypt, Libya and Jordan, and lies below 29 €/MWh$_{el}$. Turkey has on average the highest PV generation cost due to its northern location. Among the model regions with coastlines - and thus e-fuel production model regions - Jordan, Egypt, and Saudi Arabia have the lowest LCOE for PV.

The electricity generation costs of CSP are higher than those of PV, ranging from 47 €/MWh$_{el}$ to 88 €/MWh$_{el}$. The cheapest 90% of the CSP generation potential has a LCOE below 55 €/MWh$_{el}$. The regional distribution tends to show a stronger north–south gradient than PV because CSP power plants depend on direct solar irradiation. The overall cheapest 10% of the CSP potential is located in Egypt, and Libya, and lies below 49 €/MWh$_{el}$. The most expensive CSP power generation takes place in Turkey, northern Morocco, northern Algeria, and northern Tunisia. Larger areas in Turkey, Morocco, and western Saudi Arabia show no CSP potential. These areas were excluded from the potential calculation due to excessive slopes.

Compared to solar power generation technologies, wind potentials exhibit higher generation costs in 2050. The levelized cost of electricity for onshore wind ranges from 43 €/MWh$_{el}$ to well above 140 €/MWh$_{el}$. The electricity generation costs of onshore wind show stronger local differences than the solar technologies. Small, low-cost wind hotspots exist in western Morocco and eastern Egypt. Larger areas of relatively good wind sites are located in Algeria and Libya.

3.1.2. *RES potential curves*

Categorizing the LCOE shown in Fig. 6 in cost steps results in the potential curves illustrated in Fig. 7. The potential curves show the accumulated generation potential of renewable energies for increasing LCOEs in 2030 and 2050.

In Fig. 7 a) the generation potential of the renewable technologies considered is illustrated for 2030. The dominance of solar PV in MENA becomes apparent from the high generation potential of about 90,000 TWh$_{el}$ at costs below 45 €/MWh$_{el}$. At a LCOE of 60 €/MWh$_{el}$, 2,200 TWh$_{el}$ of onshore wind generation potential becomes exploitable. Solar CSP is more expensive in 2030 than other renewable technologies, such that a CSP generation potential of about 20,000 TWh$_{el}$ is available at costs of 70 €/MWh$_{el}$. The absolute CSP potential surpasses the solar PV potential at generation costs of 80 €/MWh$_{el}$ with about 90,000 TWh$_{el}$.

Fig. 7 b) shows the renewable potential curves for the MENA region in 2050. Solar PV is still the dominant technology for both spatial coverages in 2050. Due to a decrease in installation costs, the generation potential of solar PV reaches almost 99,000 TWh$_{el}$ at costs below 35

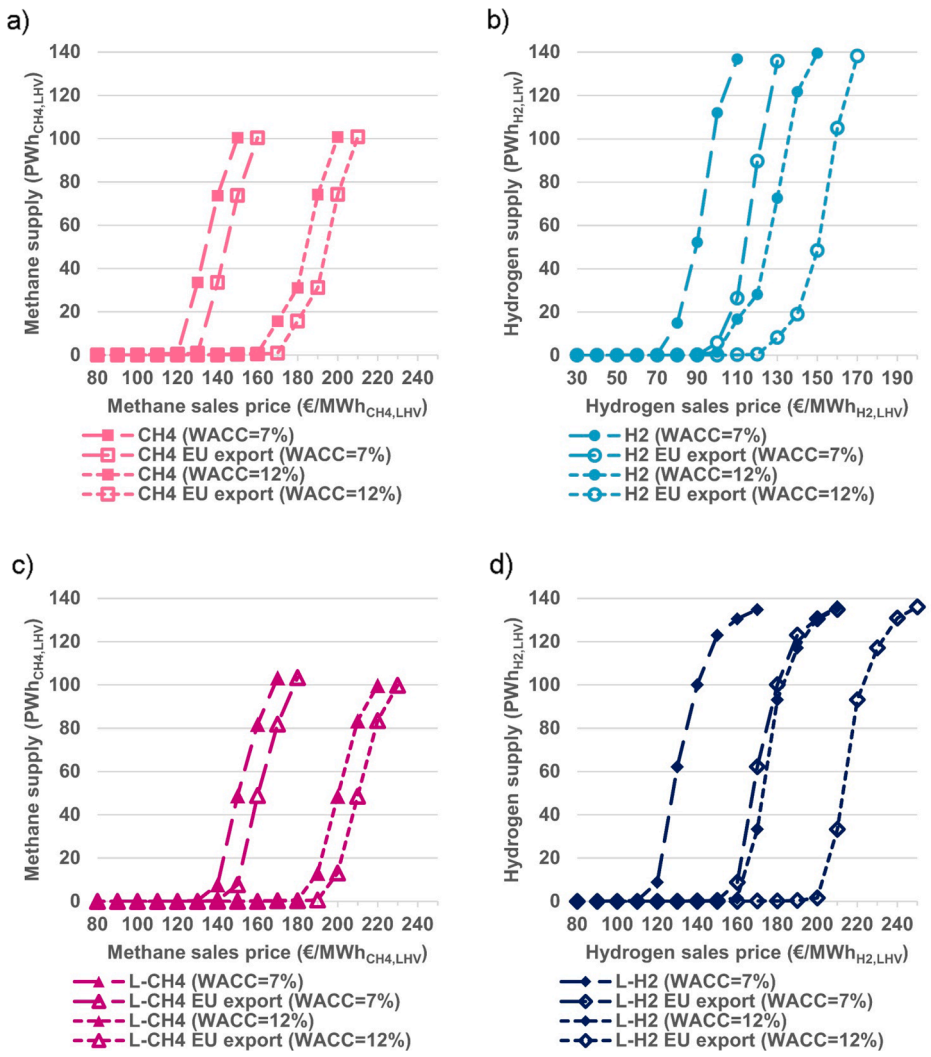

Fig. 9. Supply curves of e-fuels in the MENA region including and excluding transportation to the EU in 2050. Production and export quantities of a) methane (CH4), b) hydrogen (H2), c) liquefied methane (L-CH4), and d) liquefied hydrogen (L-H2) are shown for a weighted average cost of capital (WACC) of 7% and 12%.

€/MWh$_{el}$. This is a significant increase compared to 2030, where the generation potential of solar PV below 35 €/MWh$_{el}$ is 0 TWh$_{el}$. At LCOE of 50 €/MWh$_{el}$, CSP power plants become available with a generation potential of 32,980 TWh$_{el}$. At 55 €/MWh$_{el}$, the potential of CSP reaches the potential of solar PV and from 60 €/MWh$_{el}$, the CSP potential surpasses the solar PV potential with a generation potential of 113,000 TWh$_{el}$. At LCOE of 55 €/MWh$_{el}$, onshore wind potential of 895 TWh$_{el}$ becomes exploitable. The number of onshore wind potentials is minor compared to the combined potential of solar PV and CSP. This is due to low wind speeds in the MENA region and high solar irradiation.

Overall, the renewable power generation potential in the MENA region is enormous. A comparison with European gross energy consumption in 2018 shows that in 2050, the generation potential of solar PV alone is six times greater than the gross energy consumption of the EU 27 in 2018.

The renewable potential curves show the theoretically exploitable potential. However, these potential curves are calculated without taking into account existing or potential infrastructures. MENA countries are therefore subdivided into 250 km wide strips to account for the cost of transmission grids between regions with different renewable potentials in the *Enertile* calculations.

3.2. *E-fuel production in the MENA region*

This section shows the model results of e-fuel production in the MENA region. Due to Europe's contrasting structure, with scarce land for renewable electricity generation coupled with high energy demands, Europe is a potential trading partner for e-fuels with the MENA region. Therefore, this section also considers transportation of e-fuels to Europe. Section 3.2 shows e-fuels supply curves for the MENA region including and excluding transportation to Europe and breaks down the resulting cost components of e-fuel production. The electricity system in MENA for the production of electricity-based hydrogen and synthetic methane is described in Section 3.3. Section 3.5 discusses the competition in the European hydrogen market between imports from the MENA region and European hydrogen production.

3.2.1. *Supply curves of hydrogen and synthetic methane*

Fig. 8 and Fig. 9 show supply curves of electricity-based hydrogen and methane determined by the optimization model for the years 2030 and 2050 in the MENA region. The figures show production quantities of these electricity-based fuels for rising sales prices (as ex works prices) and at WACCs of 7% and 12%. In addition to production costs, transportation from MENA to Europe is an important cost component for evaluating the e-fuel export option to Europe. Each supply curve for MENA is therefore supplemented by an export curve to Europe, which

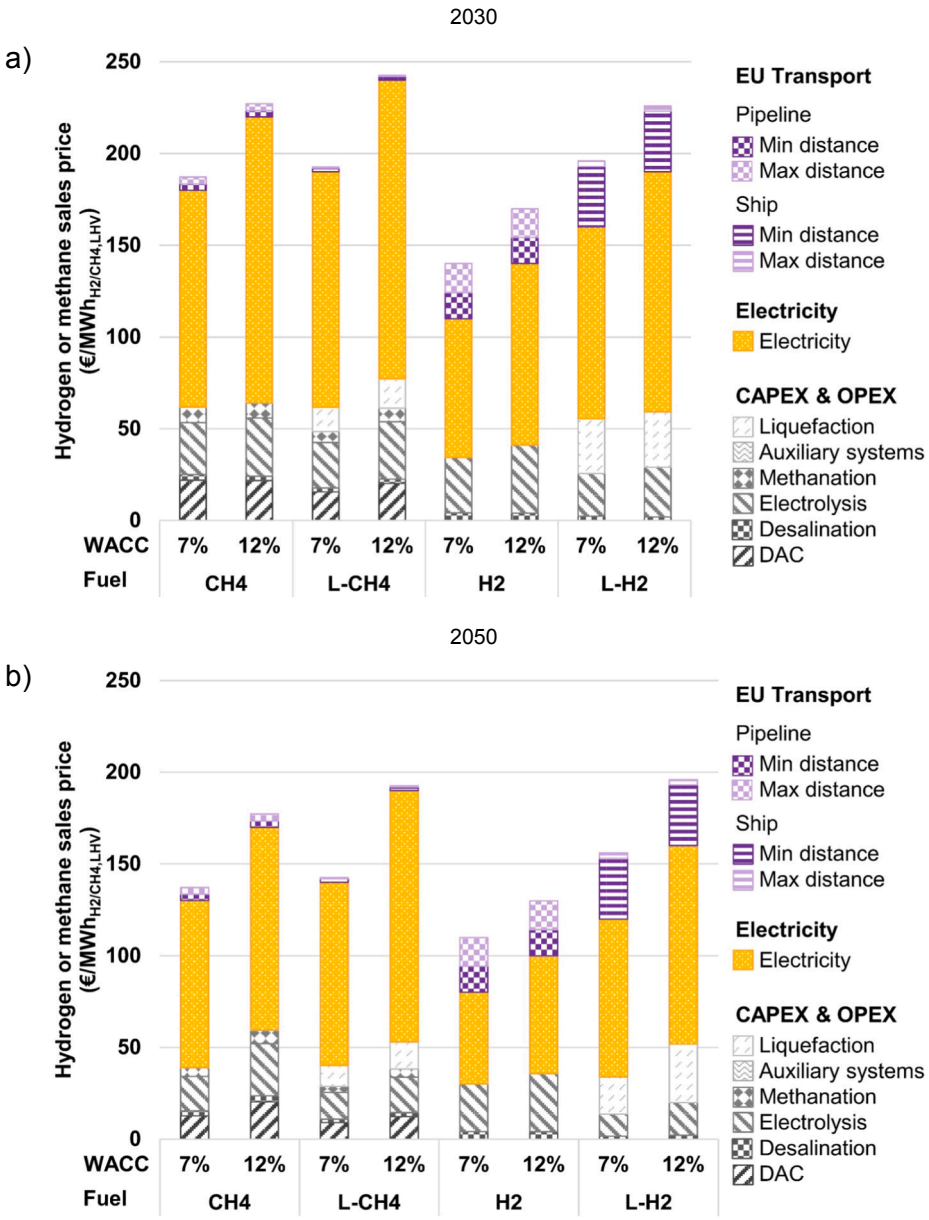

Fig. 10. Supply cost components of electricity-based hydrogen (H2), liquefied hydrogen (L-H2), methane (CH4), and liquefied methane (L-CH4) at WACC of 7% and 12% in MENA and as exports to Europe in 2030 (a) and 2050 (b). Selected points on the supply curves behind the bars have in common that the e-fuel generation volume exceeds 1,000 $TWh_{H2/CH4,LHV}$ for the first time. Consequently, bars correspond to different e-fuel production volumes. The range of transportation costs derives from minimum and maximum distances between regions centers of e-fuel production regions in MENA and the European region center.

includes transportation costs. Hydrogen and methane utilized as electricity storages within the MENA region are included in the scenario runs, but not in the supply curves. It is important to note that the curves represent techno-economic potentials but not necessarily realistic trajectories of expansion. This applies in particular to the period up to 2030, in which higher sales prices result in quantities that would be very difficult to ramp up to in less than a decade.

The optimization results in Fig. 8 and Fig. 9 show steep increases in the production quantities of electricity-based fuels with increasing sales prices in the MENA region. Depending on the interest rate, substantial hydrogen production in 2030 starts above 100 €/$MWh_{H2,LHV}$ (7% WACC) and 130 €/$MWh_{H2,LHV}$ (12% WACC). Taking into account hydrogen pipeline transport costs (cf. section 2.2.5), the supply curves of hydrogen produced in MENA for Europe start above 120 €/$MWh_{H2,LHV}$ (7% WACC) and 150 €/$MWh_{H2,LHV}$ (12% WACC). Synthetic methane is more expensive due to the additional synthesis step and the required CO_2 capture. In 2030, substantial methane production starts above sales prices of 170 €/$MWh_{CH4,LHV}$ at 7% WACC and above a sales price of 210 €/$MWh_{CH4,LHV}$ at 12% WACC. Methane pipeline transportation costs to Europe (cf. section 2.2.5) mean that the potential MENA supply of synthetic methane to Europe starts above 180 €/$MWh_{CH4,LHV}$ (7% WACC) and 220 €/$MWh_{CH4,LHV}$ (12% WACC). The spread in interest rates between model runs shows that higher interest rates not only shift the supply curves for electricity-based hydrogen and methane each to the right but also flatten their respective trajectories.

Additional liquefaction increases the costs of hydrogen and methane and shifts the supply curves of the electricity-based energy carriers further to the right. In 2030, the production of substantial amounts of liquefied hydrogen starts above a sales price of 150 €/$MWh_{H2,LHV}$ with a WACC of 7%, and above 180 €/$MWh_{H2,LHV}$ with a WACC of 12%. Substantial synthetic liquid methane production starts above a sales price of 180 €/$MWh_{CH4,LHV}$ (7% WACC). A higher WACC of 12% causes the MENA supply curve to start above 230 €/$MWh_{CH4,LHV}$.

Liquid hydrogen and liquid methane are more expensive to export to Europe than their gaseous counterparts. Although the costs of transporting liquid methane by ship are lower than those of transporting gaseous methane by pipeline for the distances considered here (see sections 2.2.5 and 3.2.2), this cannot compensate for the additional costs of liquefaction. European supply of liquid methane imported from MENA starts above sales prices of 190 €/$MWh_{CH4,LHV}$ (7% WACC) and

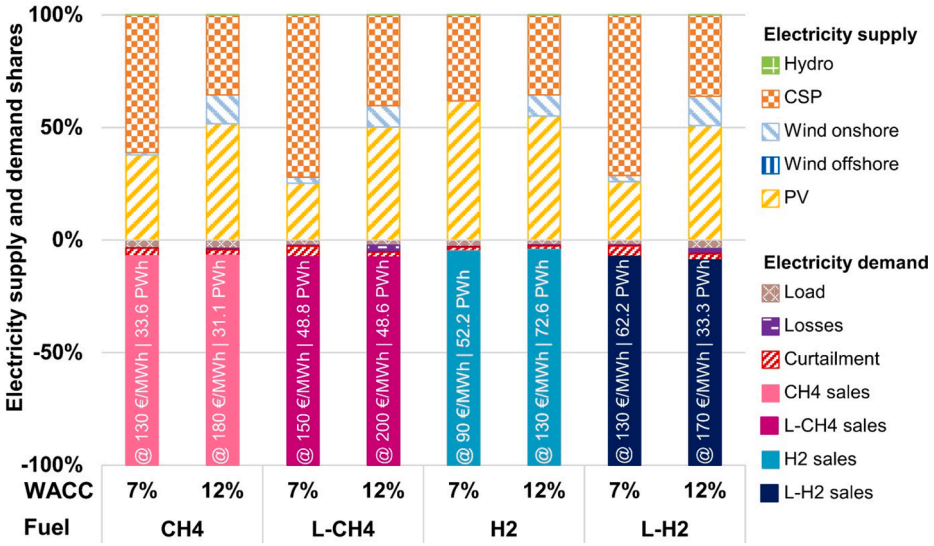

Fig. 11. Electricity generation and demand mixes in MENA in 2050. Selected bars belong to different production volumes of e-fuels, but aim at comparability of the underlying power systems.

240 €/$MWh_{CH4,LHV}$ (12% WACC). Liquid hydrogen from MENA is available in Europe above sales prices of 190 €/$MWh_{H2,LHV}$ (7% WACC) and 220 €/$MWh_{H2,LHV}$ (12% WACC).

Technological learning reduces the generation costs of e-fuels between 2030 and 2050. This cost reduction affects not only the components of the PtG process chains but also the power generation technologies. Fig. 9 shows left shifts in the supply curves for 2050 compared to 2030. Substantial hydrogen production in MENA in 2050 starts above sales prices of 70 €/$MWh_{H2,LHV}$ (7% WACC) and 90 €/$MWh_{H2,LHV}$ (12% WACC), depending on the weighted average cost of capital. Electricity-based methane is available at sales prices starting above 120 €/$MWh_{CH4,LHV}$ (7% WACC) and 160 €/$MWh_{CH4,LHV}$ (12% WACC). The additional liquefaction of hydrogen increases the generation costs by at least 40 €/$MWh_{H2,LHV}$. This shifts the start of the hydrogen supply curve for liquid hydrogen to 110 €/$MWh_{H2,LHV}$ at a WACC of 7% and to 150 €/$MWh_{H2,LHV}$ at a WACC of 12%. In the model results in 2050, substantial liquid methane production starts above 130 €/$MWh_{CH4,LHV}$ (7% WACC) and 180 €/$MWh_{CH4,LHV}$ (12% WACC).

As in 2030, exporting gaseous hydrogen and methane to Europe in 2050 is cheaper than their respective liquid forms when production and transport are taken into account. The supply of substantial amounts of gaseous hydrogen from MENA to Europe starts above a sales prices of 90 €/$MWh_{H2,LHV}$ (7% WACC) and 120 €/$MWh_{H2,LHV}$ (12% WACC). Substantial exports of gaseous methane from MENA to Europe are available starting above sales prices of 130 €/$MWh_{CH4,LHV}$ (7% WACC) and 170 €/$MWh_{CH4,LHV}$ (12% WACC).

3.2.2. *Cost components of e-fuel production*

Fig. 10 shows the cost components associated with the production of e-fuels in the MENA region for 2030 and 2050. Each bar corresponds to a point on the supply curves in section 3.2.1. Selected supply curve points exceed the hydrogen or synthetic methane production of 1,000 $TWh_{H2/CH4,LHV}$ for the first time. This choice is arbitrary, yet assumes substantial generation quantities and a strong role of the MENA region in a future global e-fuel market. The figure aims at comparability between different e-fuel production concepts. However, a direct consequence of this benchmark approach is that different e-fuel generation volumes lie behind the bars shown in the cost breakdown.

The optimization results show that renewable electricity is the most important cost component for synthetic methane production. Depending on the simulation year, physical state of the product, and assumed WACC, electricity supply accounts for between 65% and 72% of methane production (excluding transportation costs to Europe). Annuitized investments and fixed operation and maintenance costs represent the missing 28% to 35% of methane production costs in MENA. The cost of transport to Europe — accounting for between 2.0 €/$MWh_{CH4,LHV}$ and 2.7 €/$MWh_{CH4,LHV}$ via ship and between 3.5 €/$MWh_{CH4,LHV}$ and 7.3 €/$MWh_{CH4,LHV}$ via pipeline depending on the transport distance — is negligible compared to generation costs.

The technology with the highest cost contributions in methane production is electrolysis. This applies both to electricity costs, where its share is always at least 81%, and to fixed-cost components, with a share of at least 36%. Overall, electrolysis accounts for at least 69% of synthetic methane production costs without transport. The second largest cost contribution derives from CO_2 supply. It accounts for between 10% and 15% of methane production costs depending on the simulation year, physical state of the product, and assumed WACC. The cost contribution of DAC is dominated by fixed-cost components. Seawater desalination and methanation as well as intermediate compression costs lag behind those of electrolysis and DAC and are mainly fixed costs. If methane is liquefied for subsequent transport to Europe, this accounts for 8% to 10% of production cost in MENA, depending on the simulation year and assumed WACC.

The cost composition of electricity-based hydrogen depends strongly on the physical state in which it is provided. Nevertheless, electrolysis — in particular the electricity demand of the electrolysis process — remains the largest cost component in the supply of hydrogen. In the case of gaseous supply, at least 95% of the hydrogen production costs are attributable to electrolysis. At least two thirds of the electrolysis costs are electricity input; the rest are annuitized investments and fixed operation and maintenance costs. If the gaseous hydrogen is subsequently exported to Europe by pipeline, the transport costs account for 9% to 27% of the supply costs in Europe depending on the transportation distance, simulation year, and assumed WACC. If hydrogen is exported to Europe in liquid form, liquefaction and ship transport together account for a substantial part of the supply costs at 35% to 42%. However, in liquid hydrogen production — without transport — electrolysis remains the technology with the largest cost contributions in the production chain. Depending on the simulation year and assumed WACC, electrolysis accounts for between 67% and 69% of liquefied hydrogen production costs. At least 79% of the electrolysis costs are electricity costs. Desalination of seawater is a minor component compared to other process steps.

3.2.3. *Comparison of PEM-based and SOEC-based e-fuel production*

The choice of electrolyzer technology for e-fuels production in the

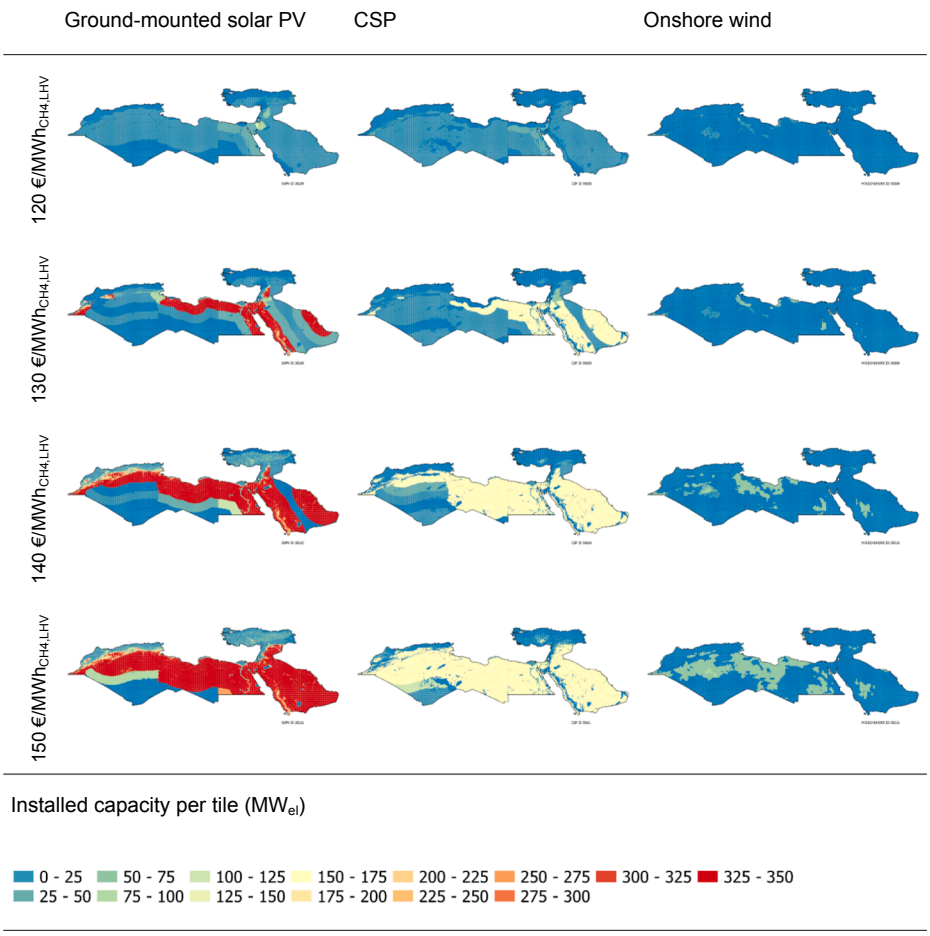

Fig. 12. Evolution of renewable electric capacities for PV, CSP, and onshore wind for gaseous synthetic methane production at rising sales prices and a weighted average cost of capital of 7% in 2050.

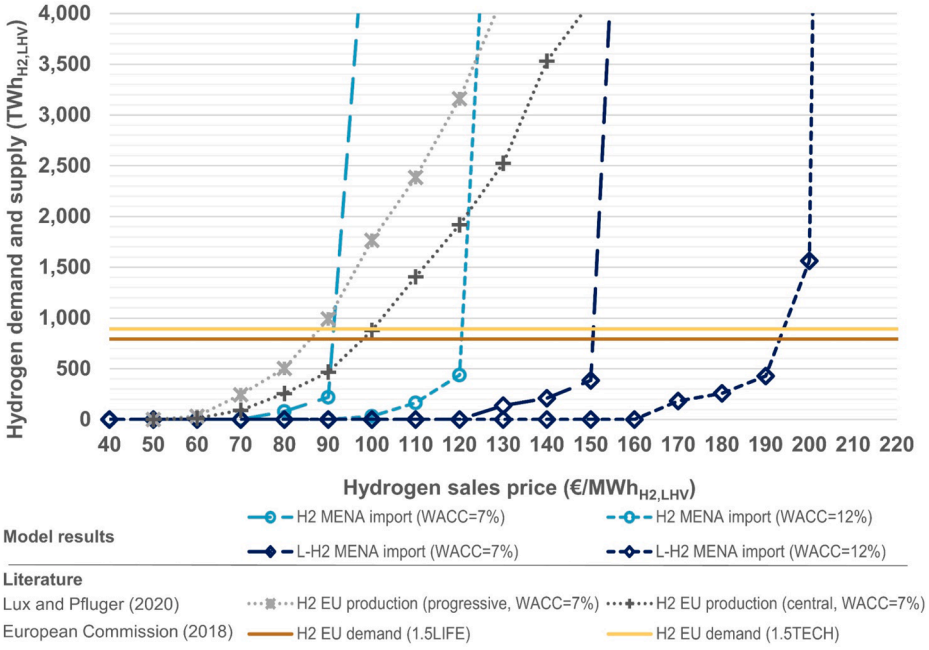

Fig. 13. Competition on the European hydrogen market in 2050. Modeled export curves from the MENA region are compared with literature values (Lux & Pfluger, 2020) for domestic European production. The hydrogen demand from the European Commission (2018a) for the year 2050 serves as a reference.

MENA region is subject to high uncertainties. In particular, the PEM and SOEC technologies considered in this article are currently at different stages of development (see section A.4). Nevertheless, it is possible to deduce techno-economic characteristics that may be decisive for the choice of electrolysis in the long term from the model results.

The model results for the year 2050 show that process chains with higher overall capital intensities rely more heavily on SOEC electrolysis. Depending on the assumed WACC, the SOEC-based process chain is used on average between 58% (7% WACC) and 82% (12% WACC) for liquid hydrogen production in 2050. For liquid methane production, the average use of the SOEC chain ranges from 61% (7% WACC) to 85% (12% WACC). In the model results, the SOEC chains achieve high full load hours of over 7,500 h per year regardless of the final product. Overall, capital-intensive process chains therefore benefit from the higher efficiency of SOEC and allocate fixed-cost components over many operating hours.

In contrast, for the production of gaseous hydrogen and methane, the model focuses on the PEM-based process chains. Depending on the assumed WACC, the PEM-based process chain is used on average between 72% (7% WACC) and 75% (12% WACC) for the production of gaseous hydrogen in 2050. For gaseous methane production, the average use of the PEM chain ranges from 52% (7% WACC) to 59% (12% WACC). The full load hours of the PEM chains lie between 2,700 and 4,000 h per year, depending on the final product. Overall, less capital-intensive process chains are therefore less dependent on the higher efficiency of SOEC and instead rely on the lower fixed costs of PEM.

3.3. Electricity system for e-fuel production in the MENA region in 2050

Fig. 11 shows the optimization result of electricity supply and demand compositions for selected points on the e-fuel supply curves for 2050. The selection of the points aims at substantial e-fuel generation quantities and electricity supply that is as comparable as possible. Consequently, the e-fuel generation quantities behind the bars differ.

On the demand side, Fig. 11 shows that due to the very high renewable electricity generation potential in the MENA region, the normal load of the MENA countries can potentially be exceeded by a multiple of electricity input for e-fuel generation. For the selected points on the supply curves, the electricity demand for e-fuel production is at least 91% of the total electricity demand. The amount of curtailed electricity in the optimization results is small overall with a maximum of 5% in the case of liquefied hydrogen and a WACC of 12%.

The supply side is dominated by solar generation technologies for all e-fuels and configurations studied. At a WACC of 7%, PV and CSP account for between 97% and 100% of the electricity generation mix. Increasing the WACC from 7% to 12% leads to an increase in the onshore wind share of electricity generation for all four electricity-based energy carriers considered (hydrogen, liquefied hydrogen, synthetic methane, and liquefied synthetic methane). However, the proportion of wind in the electricity mix remains comparatively low with a maximum of 13% for gaseous methane production.

Higher capital intensity in the production of electricity-based fuels increases the share of CSP in the electricity generation mix. Firstly, this can be seen when comparing hydrogen and methane production. The additional synthesis step and technical equipment used in methane production increase the capital intensity compared to similar production routes for electricity-based hydrogen. This leads to higher CSP shares in each case. Secondly, additional liquefaction in particular increases the capital costs of the overall process chains compared to gaseous supply. In the optimization result, liquefaction and the associated increase in capital intensity leads to an increase in the CSP share compared to the gas-based generation routes. This effect can be explained by the higher full load hours of electricity production of CSP compared to PV. The thermal intermediate storage of energy in CSP allows higher investments to be allocated to more operating hours of the PtG process chains.

In the energy systems in Fig. 11, the model uses battery storages in 400 to 900 h of a year to increase the full load hours of the PtG generation plants. Battery storage systems exhibit higher utilization in calculations with a WACC of 12%. The batteries allow fixed-cost components of the PtG plants, which are more pronounced at a WACC of 12%, to be allocated to more operating hours.

3.4. Regional distribution of e-fuel supply

Fig. 12 shows the evolution of the renewable energy expansion along the supply curve of gaseous synthetic methane at a WACC of 7% for the year 2050. In the optimization results, synthetic methane generation starts with small production quantities at a selling price of 120 €/$MWh_{CH4,LHV}$ in Egypt (439 $TWh_{CH4,LHV}$), Saudi Arabia (219 $TWh_{CH4,LHV}$), Jordan (71 $TWh_{CH4,LHV}$), and Morocco (61 $TWh_{CH4,LHV}$). The division of the MENA countries into sub-regions, where e-fuels can only be generated in the coastal regions and electricity generation in the hinterland is subject to grid penalties, results in a gradual exploitation of the electricity generation potential in the hinterland. This happens despite the flat generation cost structure of renewable energies shown in section 3.1. The coloring of the maps shows that at a sales price of 130 €/$MWh_{CH4,LHV}$ methane production is expanded by the optimizer. The first substantial synthetic methane quantities are produced especially in Saudi Arabia (16,404 $THW_{CH4,LHV}$), Egypt (9,269 $THW_{CH4,LHV}$), Libya (5,650 $THW_{CH4,LHV}$), and Morocco (1,006 $THW_{CH4,LHV}$). This results in a roll-out of PV in the coastal regions and the build-up of CSP capacities, which already reach further inland. The expansion of onshore wind power at this methane sales price is limited to the aforementioned individual hotspots in Morocco, Libya, and Egypt. At a methane sales price of 150 €/$MWh_{CH4,LHV}$, the model results are dominated by high power densities for CSP and PV outside of Turkey, Lebanon, and Israel.

Distance-dependent cost premiums for pipeline transport of synthetic methane from MENA to Europe do not change the order of the first exporting countries given the accuracy of our result resolution. Assuming a WACC of 7%, the first substantial exports of gaseous synthetic methane to Europe in 2050 start at a selling price of 140 €/$MWh_{CH4,LHV}$ from Saudi Arabia (16,404 $TWh_{CH4,LHV}$), Egypt (9,269 $TWh_{CH4,LHV}$), and Libya (5.650 $TWh_{CH4,LHV}$).

The first substantial hydrogen production quantities for the MENA region and a WACC of 7% appear in the model results at a sales price of 80 €/$MWh_{H2,LHV}$. At this sales price hydrogen is mainly produced in Saudi Arabia (5,030 $TWh_{H2,LHV}$), Egypt (4,132 $TWh_{H2,LHV}$), and Libya (3,854 $TWh_{H2,LHV}$). Based on our measurement accuracy and using distance-based cost premiums for pipeline transport of gaseous hydrogen from MENA to Europe, the order of exporting countries changes at the beginning of the supply curve. The first substantial hydrogen volumes are provided in Europe at a sales price 100 €/$MWh_{H2,LHV}$ from Libya (3,854 $TWh_{H2,LHV}$) and Morocco (910 $TWh_{H2,LHV}$). Due to the further distance, Saudi Arabia exports substantial amount of hydrogen (5,030 $TWh_{H2,LHV}$) to Europe only starting at a selling price of 110 €/$MWh_{H2,LHV}$.

3.5. Competition on the European hydrogen market

One criterion for deciding whether hydrogen from the MENA region can become part of the European supply mix is the relationship between the supply costs of European hydrogen and hydrogen imported from MENA.

Fig. 13 shows a comparison of the supply costs of hydrogen in Europe, which is either produced in Europe itself or imported from MENA. The supply curves of a European production are taken from Lux and Pfluger (2020). In general, the modeling approach used to calculate European supply curves and the MENA import curves is similar. However, since Lux and Pfluger (2020) was published, there has been a cost update for renewable electricity generation technologies in *Enertile*. The update has resulted in structurally lower renewable electricity

generation costs. The European hydrogen supply curves in Fig. 13 are therefore subject to higher electricity production costs than the hydrogen import curves from the MENA region. A second difference between the model parameterizations in Lux and Pfluger (2020) and scenario runs in this article applies to the used techno-economic data for electrolyzers[5]. In both cases MENA import and European production costs for the local distribution of hydrogen are not considered.

The comparison of the model results shows that the import curves remain below the European supply curves up to a hydrogen price of 90 €/$MWh_{H2,LHV}$. Up to this sales price and corresponding hydrogen quantities, domestic-European hydrogen supply is more cost-efficient. Assuming the same WACC of 7% for Europe and MENA, the import of gaseous hydrogen from the MENA region becomes economically attractive starting at hydrogen demands between 488 $TWh_{H2,LHV}$ and 1,118 $TWh_{H2,LHV}$, depending on the electrolyzer parametrization in Lux and Pfluger (2020). If the import of hydrogen is subject to substantially higher risk premiums or profit margins realized in the model runs by a WACC of 12%, the import of hydrogen is only profitable compared to domestic European production starting above hydrogen quantities between 2,044 $TWh_{H2,LHV}$ and 3,571 $TWh_{H2,LHV}$. The intersection of the supply curves for liquid hydrogen imports from MENA with the European supply occurs above hydrogen sales prices of 150 €/$MWh_{H2,LHV}$ and European hydrogen supplies of 4,111 $TWh_{H2,LHV}$.

In compliance with the 1.5 °C target, the long-term strategic vision of the EC estimates a final energy demand for hydrogen in Europe in 2050 between 794 TWh_{H2} (1.5LIFE scenario) and 892 TWh_{H2} (1.5TECH scenario) (European Commission, 2018a). The comparison of hydrogen supply curves between European production with the central electrolyzer parametrization and MENA imports in Fig. 13 implies that, from a techno-economic point of view, these demands could be partly met by MENA imports, if Europe and MENA are subject to the same interest rates. For the progressive electrolyzer parametrization in Europe and a WACC of 7% hydrogen demands could be met cost efficiently by an inner European production. If MENA imports are assigned a higher WACC of 12%, these European hydrogen demands would be met by domestic European hydrogen production independently of the electrolyzer parameter scenario in Europe. However, imports could also be necessary if the RES potential in Europe cannot be sufficiently utilized due to lack of public acceptance.

4. Summary & conclusions

This article identifies the generation potentials of the electricity-based fuels hydrogen and synthetic methane for the MENA region in 2030 and 2050. For the generation of these e-fuels, it is assumed that only renewable electricity is used. The analysis is performed with the energy system optimization model *Enertile*. Based on the model results, the export of e-fuels from MENA to Europe is also considered using distance dependent transport costs.

The energy system optimization in *Enertile* is based on an assessment of renewable electricity potentials in the MENA region at high resolution. The resulting cost potential curves and the distribution of the considered renewable technologies show that PV and CSP are the most cost-efficient technologies in the MENA region. The wind potential in the MENA region lags behind solar technologies in its suitability for producing e-fuels. Electricity generation by wind at low cost is limited to individual hot spots on the coast and in some inland areas. Cheap renewable power generation potentials in coastal areas are located in Egypt, Saudi Arabia, Libya, and Morocco. Following the scenario architecture, which postulates that e-fuels are only produced in coastal regions, these countries make the first and least expensive contributions to e-fuel production in the model calculations.

The cost potential curves are calculated for two different assumptions regarding the weighted average cost of capital (WACC), 7% and 12%. The model results for the generation of e-fuels show that substantial amounts of gaseous hydrogen can be produced in MENA in 2030 starting above a production cost of 100 €/$MWh_{H2,LHV}$ (7% WACC) and 130 €/$MWh_{H2,LHV}$ (12% WACC). In 2050, the start of the hydrogen supply curves drops to above 70 €/$MWh_{H2,LHV}$ (7% WACC) and 90 €/$MWh_{H2,LHV}$ (12% WACC). As the supply curves progress, they show a steep increase in production volumes. Additional liquefaction increases hydrogen supply cost by at least 40 €/$MWh_{H2,LHV}$.

Due to the additional synthesis step and the required CO_2 capture, the production of synthetic methane is more expensive than electricity-based hydrogen. In the model results, a substantial gaseous methane production in 2030 starts above a generation cost of 170 €/$MWh_{CH4,LHV}$ (7% WACC) and 210 €/$MWh_{CH4,LHV}$ (12% WACC) in MENA. In 2050, the model results show substantial synthetic methane generation volumes above generation costs of 120 €/$MWh_{CH4,LHV}$ (7% WACC) and 160 €/$MWh_{CH4,LHV}$ (12% WACC). The supply curve of methane also shows a steep increase for rising sales prices. Additional liquefaction increases the cost of synthetic methane by at least 10 €/$MWh_{CH4,LHV}$.

A cost comparison shows that exporting gaseous hydrogen and methane to Europe is cheaper than transporting their respective liquid forms. Taking into account methane pipeline transportation costs to Europe, the potential MENA supply of synthetic methane from MENA to Europe starts above 180 €/$MWh_{CH4,LHV}$ (7% WACC) and 220 €/$MWh_{CH4,LHV}$ (12% WACC) in 2030. Equivalent export curves of hydrogen produced in MENA for Europe start above 120 €/$MWh_{H2,LHV}$ (7% WACC) and 150 €/$MWh_{H2,LHV}$ (12% WACC). In 2050, exports of gaseous methane from MENA to Europe are available starting at sales prices above 130 €/$MWh_{CH4,LHV}$ (7% WACC) and 170 €/$MWh_{CH4,LHV}$ (12% WACC). The supply of hydrogen produced in MENA for Europe in 2050 starts at sales prices above 90 €/$MWh_{H2,LHV}$ (7% WACC) and 120 €/$MWh_{H2,LHV}$ (12% WACC), respectively.

The cost of renewable electricity is decisive for e-fuel production costs, accounting for at least 62% of e-fuel generation costs in the production chains examined. For both hydrogen and synthetic methane production, the technology with the highest cost contributions is electrolysis. Regardless of the simulation year and assumed WACC, electrolysis accounts for at least 95% of gaseous hydrogen production costs and at least 69% of the costs in synthetic methane production. The second major cost component in methane production is CO_2 supply from ambient air. It accounts for 10% to 15% of generation costs, depending on the physical state of the product, simulation year, and assumed WACC. The remaining plant components, seawater desalination and methanation, are less prominent in the overall costs. Cost reductions between the simulation years 2030 and 2050 are due to lower costs for renewable electricity and technical learning of the e-fuel production chains.

The production of electricity-based renewable gases is characterized by the large and low-cost solar power generation potentials in the MENA region. PV and CSP account for at least 87% of the electricity mix for e-fuel production in all constellations studied. Increasing capital intensity by liquefying or processing hydrogen into methane increases the share of CSP in the generation mix, due to its relatively high full load hours in electricity generation. Wind energy plays a relatively small role in e-fuel generation in MENA. The maximum share of onshore wind in the generation mix of the MENA region is 13% in the model results.

The comparison of the calculated hydrogen supply in the MENA region with equivalent supply curves in Europe shows that hydrogen trade flows from MENA to Europe can only be cost-efficient within certain limits. In order to have hydrogen export flows from MENA to Europe in a competitive market context, the following two conditions need to be met. Firstly, there is no interest rate spread or only a low interest rate spread between Europe and the MENA countries. This

[5] In Lux and Pfluger (2020), hydrogen supply curves are calculated for three different techno-economic parameterizations of PEM electrolyzers. The conservative version of the electrolysis parameters is not shown in this graph, because it lacks comparability with the parameterization for the MENA region.

means that investors are willing to develop projects in MENA at similar financing conditions as in Europe. Secondly, the transportation costs for hydrogen are low. Transportation costs by pipeline account for a substantial proportion of hydrogen supply costs from MENA in Europe. In the current literature, these transportation costs are characterized by large spreads and uncertainties. Apart from this, an effective shortage of sites for expanding renewable electricity generation in Europe could be a game changer and may lead to hydrogen imports from MENA. This may arise, for example, from high electricity demands accompanied with low acceptance for a widespread expansion of renewable electricity generation units in Europe.

The analysis also has relevance for policy decisions: First of all, it broadens the perspective regarding the costs of e-fuel imports: Several previous publications use somewhat simplified assumptions, for example regarding the price of electricity used in hydrogen production, or assume very low interest rates. The more holistic framework used in this analysis provides a more comprehensive picture of the costs incurred. The higher costs resulting from this show that importing e-fuels to Europe is not a cheap silver bullet to circumvent bottlenecks in renewable energy expansion or achieve supply side transformation. The cost of e-fuels have to be weighed up against other options. The analysis also hints at certain regions that might be most suitable for producing e-fuels for exports. However, the differences in site quality vary within a range, in which other factors might be equally important, such as transport costs and interest rate expectations for individual countries or even projects.

Analyzing e-fuel production chains in detail and considering transport also highlights the complexity and sheer size of these potential projects. Too often hydrogen and e-fuel imports are used as the gap-filler in national energy transformation strategies. The deeper analysis shows that these projects are too large and too costly to happen without strong policy support and without high security that the energy products will be bought long-term at agreed prices. Policy makers aiming at importing hydrogen or e-fuels should start developing policies in this direction soon, as infrastructure projects of the sizes discussed here have a considerable lead time.

Overall, the analysis shows that e-fuel production in the MENA region is indeed attractive, especially due to its high solar potential. However, the question of whether utilizing this potential for Europe's energy supply makes sense from a strictly economic point of view is not answered definitively. Differences in capital costs and transport costs may reduce or even nullify the advantages of the region. Future analysis should analyze these aspects in even greater detail and take price formation on international energy commodity markets into account.

CRediT authorship contribution statement

Benjamin Lux: Conceptualization, Methodology, Investigation, Visualization, Data curation, Writing – original draft, Writing – review & editing. **Johanna Gegenheimer:** Data curation, Writing – original draft, Writing – review & editing. **Katja Franke:** Methodology, Writing – original draft, Writing – review & editing. **Frank Sensfuß:** Supervision. **Benjamin Pfluger:** Conceptualization, Writing – original draft, Writing – review & editing, Supervision.

Declaration of Competing Interest

The authors declare that they have no known competing financial interests or personal relationships that could have appeared to influence the work reported in this paper.

Acknowledgments

The main content of the paper is closely related to the research work in the project MethQuest, which received funding from the Federal Ministry for Economic Affairs and Energy on the basis of a decision by the German Bundestag.

For contribution of their extensive experience with Power-to-Gas technologies, the authors thank the following project partners of MethQuest/MethFuel:

- Elogen.
- EIfER - European Institute for Energy Research.
- Karlsruhe Institute of Technology, Engler-Bunte-Institute, Division of Fuel Technology.
- Technical University of Berlin - The Electrochemical Energy, Catalysis and Material Science Group.

The authors also gratefully acknowledge Frank Graf, Friedemann Mörs and Janina Leiblein from the DVGW Research Center at Engler-Bunte-Institut of Karlsruhe Institute of Technology (KIT) for sharing their extensive knowledge in the field of Power-to-Gas and for their valuable comments.

Funding

This work was supported by funding of the German Federal Ministry for Economic Affairs and Energy [O20E-100335368].

Appendix

Abbreviations

(See Table A1)

Table A1
Abbreviations.

Abbreviation	Explanation
BEV	Battery electric vehicles
BoL	Begin of life
CAPEX	Capital expenditure
CH_4	Methane
CO_2	Carbon dioxide
CSP	Concentrating solar power
DAC	Direct air capture, CO_2 separation from ambient air
EC	European Commission
EU	European Union
e-fuels	Electricity-based fuels
el	electrical
FLH	Full load hours
GHG	Greenhouse gas
H_2	Hydrogen
L-hydrogen	Liquefied hydrogen
L-methane	Liquefied methane
LCOE	Levelized cost of electricity
LHV	Lower heating value
LNG	Liquefied natural gas
MENA	Middle East and North Africa
O&M	Operation and maintenance cost
OPEX	Operating expenditure
PEMEL	Polymer electrolyte membrane electrolysis
PtG	Power-to-Gas
PtH_2	Power-to-Hydrogen
$PtCH_4$	Power-to-Methane
PtX	Power-to-X
PV	Photovoltaics
RES	Renewable energy source
SED	Specific energy demand
STP	Standard temperature and pressure ($T_{STP} = 0\ ^\circ C$, $p_{STP} = 1.01325$ bar).
SOEL	Solid oxide electrolysis
th	thermal
TRL	Technology readiness level
WACC	Weighted average cost of capital
wt	weight

Substance data

(See Table A2)

Table A2
Substance data.

Substance data		
Density of water (at 0 °C)	999.8	kg/m^3
Higher heating value (HHV) of natural gas	50.0	MJ/kg
HHV of H_2	141.8	MJ/kg
Lower heating value (LHV) of H_2	120.0	MJ/kg
HHV of CH_4	55.5	MJ/kg
LHV of CH_4	50.0	MJ/kg
Molar mass of H_2	2.0	g/mol
Molar mass of CH_4	16.0	g/mol
Molar mass of water	18.0	g/mol
Molar volume at standard temperature and pressure (STP)	22.4	m^3/kmol

Model regions and transport distances to Europe

(See Fig. A1 and Table A3)

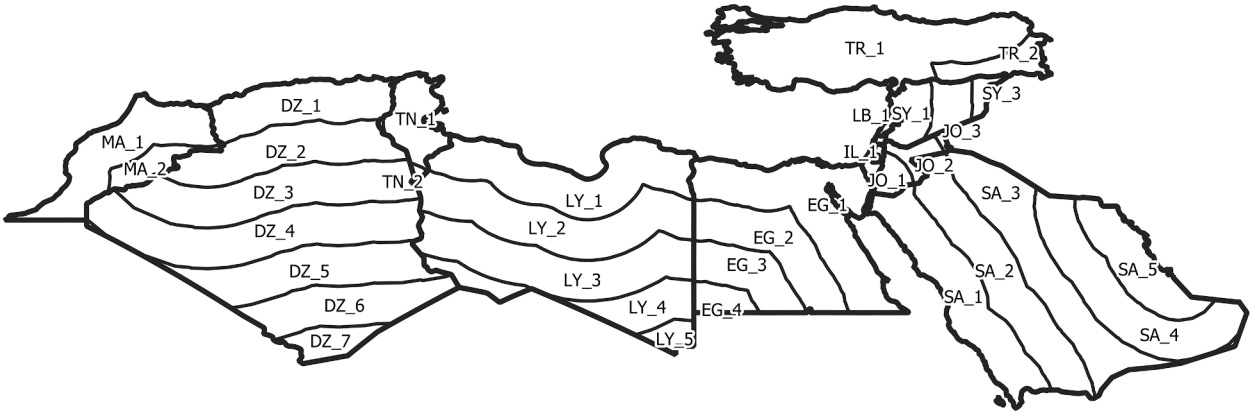

Fig. A1. Model regions for *Enertile* calculations in the MENA region.

Table A3
Transport distances assumed between e-fuel production regions in MENA and Europe. Transport distances are estimated by the center-to-center air distance of MENA and continental Europe. In reality, transport routes are likely to be different.

Transport distances from e-fuel production regions in MENA to Europe		
DZ_1	2,098	km
EG_1	3,143	km
IL_1	2,981	km
JO_1	3,119	km
LB_1	2,788	km
LY_1	2,507	km
MA_1	2,778	km
SA_1	3,988	km
SA_5	4,344	km
SY_1	2,790	km
TN_1	2,073	km
TR_1	2,232	km

Technologies and techno-economic parameters of PtG process chains

This section covers details of individual PtG technologies within the e-fuel production chains presented in section 2.2.4. Table A4 shows the specific energy demands of individual PtG technologies. Table A5 and Table A6 show specific investments and fixed operation and maintenance cost of individual PtG technologies.

Water electrolysis, in which water is electrochemically divided into hydrogen and oxygen, is the main process step for hydrogen production. This paper examines PEMEL and SOEL systems, which differ for example in the type of membrane used and the operating conditions (Adolf et al., 2017; Golling, Heuke, Seidl, & Uhlig, 2019; Smolinka et al., 2018; Töpler & Lehmann, 2016; Ursua, Gandia, & Sanchis, 2012). Fig. 4 and Fig. 5 in section 2.2.4 specify the operating temperatures and pressures, chosen for the techno-economic parametrization. As SOEL operates with steam, thermal energy is required at approximately 200 °C for water evaporation. This makes SOEL particularly promising when heat is available at the site. However, PEMEL offers the advantage of operating over a wide load range (Smolinka et al., 2018) and allows a quick response to power fluctuations from RES. PEMEL has already reached a high technology readiness level (TRL) of 9. SOEL is a newer technology (TRL 6) and its development is therefore associated with greater opportunities but also with higher risks (Golling et al., 2019). According to the literature, further optimization of PEMEL and SOEL, e. g. of cell and stack design, will lead to an increase in efficiency over the next 30 years (Smolinka et al., 2018). Efficiencies of electrolyzers given in the literature usually refer to begin of life (BoL). For the *Enertile* parametrization, efficiency reduction for PEMEL and SOEL due to stack degradation is taken into account through the author's own estimations, based on technical key data from the literature (Smolinka et al., 2018) (cf. Table A4). Accordingly, replacement of the stacks over the system lifetime of 20 years is included in the fixed OPEX (Table A6).

Currently commercially available electrolysis processes require freshwater as feedstock. In the arid MENA region, freshwater is a scarce resource (Hamed et al., 2018). In coastal regions, however, seawater is available. Electrolysis processes that directly use seawater are the subject of current research, but are only at the laboratory testing stage and are not yet commercially available (d'Amore-Domenech & Leo, 2019). To avoid competition for scarce freshwater in the MENA region and to take advantage of electrolysis technologies already available, seawater desalination is explicitly included in the economic and energy modeling and assessment of e-fuel process chains in this paper (cf. Table A4, Tables A5 and A6). Various seawater desalination technologies are commercially available today. The most commonly used desalination technology is reverse osmosis (Zhou & Tol, 2005). It has a TRL of 9 (Zhou & Tol, 2005). It is used, for example, on a large scale to provide drinking water in Israel (Atkinson, 2005). The transport of water from the coastline to the PtG site is not explicitly considered in this work, since transport costs for water are comparably low (Zhou & Tol, 2005) and PtG production sites are located close to the coast in the modeling approach.

Due to the arid climate, the MENA region offers a low potential for

Table A4
Specific electrical (el) and thermal (th) energy demand (SED) for all technologies investigated for electricity-based hydrogen and methane production in MENA. Values refer to the years 2030 and 2050.

Process step	Specific energy demand					Source	
	Electrical (el)		Thermal (th)				
	in 2030	in 2050	in 2030	in 2050			
Sea water desalination	5.5	5.5	None	None	$kW_{el}/(m^3/h$ purified water)	(Hafez & El-Manharawy, 2002)	
PEMEL	5.0	4.5	None	None	$kW_{el}/(m^3/h\ H_2$ STP)	(Smolinka et al., 2018)	a,b,c
SOEL	3.9	3.8	0.4	0.4	$kW_{el/th}/(m^3/h\ H_2$ STP)	(Smolinka et al., 2018)	bb
DAC	1.0	1.0	2.9	2.9	$kW_{el/th}/(m^3/h\ CO_2$ STP)	(Viebahn et al., 2019)	
H_2 compression from 9 to 20 bar	0.03	0.03	None	None	$kW_{el}/(m^3/h\ H_2$ STP)		a
CO_2 compression from 1 to 20 bar	0.15	0.15	None	None	$kW_{el}/(m^3/h\ CO_2$ STP)		a
H_2 liquefaction	6.76	6.02	None	None	$kW_{el}/(kg/h\ H_2)$	(Stolzenburg et al., 2013)	
CH_4 liquefaction	0.7	0.7	None	None	$kW_{el}/(kg/h\ CH_4)$	(Wärtsilä Corporation, 2016)	

a) Own estimations, taking into account degradation of the stacks by 3 µV/h for 2030 and 2 µV/h for 2050.
b) Own estimations, taking into account degradation of the stacks by 7 µV/h for 2030 and 4 µV/h for 2050.
c) The efficiency of PEMEL is not expected to increase significantly by 2030, because PEMEL electrolysis is in an economic "race to catch up" with alkaline electrolysis. Low CAPEX is prioritized over an increase in efficiency in the development of PEMEL (Smolinka et al., 2018).

Table A5
Specific CAPEX for each process step for production of electricity-based hydrogen or methane in terms of plant capacity. Values refer to plant capacities of 100 MW (LHV) hydrogen or methane output.

PtG process step	Specific CAPEX			Source	
	in 2030	in 2050			
Sea water desalination	97	97	€/(l/h fresh water out)	(Hafez & El-Manharawy, 2002)	a
PEMEL	2,000	1,800	€/(m^3/h STP H_2 out)	(Smolinka et al., 2018)	b, c
SOEL	2,912	2,002	€/(m^3/h STP H_2 out)	(Smolinka et al., 2018)	b, c
H_2 compression (9 to 20 bar)	96	none	€/(m^3/h STP H_2 in)	(Chardonnet et al., 2017)	b, c, d
Direct air capture	8,344	5,574	€/(m^3/h STP CO_2 out)	(Siegemund et al., 2019)	b, c
CO_2 compression (1 to 20 bar)	238	238	€/(m^3/h STP CO_2 in)	(Schäffer, Ortloff, Lubenau, Imberg, & Senner, 2019)	b, c
Catalytic methanation	2,778	1,815	€/(m^3/h STP CH_4 out)	(Zauner et al., 2019)	b, c, e
H_2 liquefaction	35,510	35,510	€/(kg H_2 out)	(Hank et al., 2020b)	b, c
CH_4 liquefaction	7,265	7,265	€/(kg CH_4 out)	(Songhurst, 2018)	b

a) Lifetime 15 years
b) Lifetime 20 years
c) And own estimations
d) Only necessary for PtG chain with SOEL
e) Product gas cleaning included

biomass and industry that is only located at coastal areas. For this reason, the use of ambient air as a CO_2 source is obvious (Fasihi, Efimova, & Breyer, 2019). Otherwise, CO_2 can be captured from point sources elsewhere and transported to the e-fuel production site, which is not considered in this paper. Fasihi et al. (2019) give an overview of different process concepts for the separation of CO_2 from ambient air, so-called Direct Air Capture (DAC). Climeworks GmbH supplies a DAC technology with a relatively high TRL (6 – 9), which is based on the chemisorptive binding of CO_2 molecules to amine-activated cellulose (adsorption) at ambient conditions (40 °C, 1 bar) (Viebahn, Scholz, & Zelt, 2019). At temperatures of approximately 100 °C and vacuum conditions, CO_2 is released again (desorption) and can be fed to the methanation process as an enriched CO_2 gas flow (Fasihi et al., 2019; Mörs, Schlautmann, Gorre, & Leonhard, 2020; Viebahn et al., 2019). The technology has been tested in several pilot plants, for example at the PtG demo site at Troia within the EU project STORE&GO (Mörs et al., 2020). Based on the experience gained in these projects, a further reduction of thermal SED as well as CAPEX and OPEX is expected in the next decade (Table A4, Table A5 and Table A6).

Before methanation, the reactants (hydrogen and CO_2) must first be brought to operating pressure. Table A4 shows the SED for intermediate compression of CO_2 (1 to 20 bar) and hydrogen (9 to 20 bar). In the case of PEMEL, hydrogen exits the electrolysis system at a pressure above 20 bar and hydrogen compression is not necessary. The same assumption applies to SOEL in the year 2050.

In catalytic methanation, CO_2 and hydrogen are converted to methane and water. Water can be recycled into the electrolysis, thus reducing the seawater requirement. The methanation is exothermic and releases heat of reaction (165 kJ/mol) at a relatively high temperature level (250 to 500 °C) (Götz et al., 2016; Rönsch et al., 2016; Schildauer & Biollaz, 2016). The released thermal energy can either be supplied to the DAC or used to generate steam if SOEL is chosen. For the *Enertile* parametrization, a decrease in methanation costs is assumed over the next decades. The assumed CAPEX and fixed OPEX for methanation are based on learning curves from the literature (Zauner, Böhm, Rosenfeld, & Tichler, 2019) and the author's own estimations, including costs for product gas cleaning (Table A5 and Table A6).

For methane liquefaction, a relatively high amount of energy is required to cool the gas below the boiling temperature (-162 °C, 1 bar) and to remove the enthalpy of condensation (Table A4). The energy density is thus increased by a factor of 600 (approx. 5.6 MWh_{CH4}/m^3) compared to ambient temperature. Methane liquefaction is well known as an application for natural gas transport, so no further cost reduction is assumed (Table A5 and Table A6).

The energy demand for hydrogen liquefaction is over three times higher than for methane, related to LHV, due to the low boiling temperature of -253 °C (Table A4). The optimization of hydrogen liquefaction is part of current research (Stolzenburg et al., 2013) and development work, so reduction in SED and costs is expected in the medium term (Table A5 and Table A6).

Table A6
Specific OPEX for each process step for production of electricity-based hydrogen or methane; costs for electricity and heat excluded; in terms of plant capacity; referring to plant capacity of 100 MW (LHV) hydrogen or methane output.

PtG process step	Specific fixed OPEX			Source	
	in 2030	in 2050			
Sea water desalination	19	19	€/(l/h fresh water out)/a	(Hafez & El-Manharawy, 2002)	
PEMEL	37	31	€/(m^3/h STP H_2 out)/a	(Smolinka et al., 2018)	a
SOEL	187	77	€/(m^3/h STP H_2 out)/a	(Smolinka et al., 2018)	b
H_2 compression (9 to 20 bar)	Neglected	Neglected	€/(m^3/h STP H_2 in)/a		
Direct air capture	167	111	€/(m^3/h STP CO_2 out)/a	(Siegemund et al., 2019)	
CO_2 compression (1 to 20 bar)	Neglected	Neglected	€/(m^3/h STP CO_2 in)/a		
Catalytic methanation	100	66	€/(m^3/h STP CH_4 out)/a	(Zauner et al., 2019)	c
H_2 liquefaction	1,420	1,420	€/(kg H_2 out)/a	(Hank et al., 2020b; Stolzenburg et al., 2013)	
CH_4 liquefaction	437	437	€/(kg CH_4 out)/a	(Songhurst, 2018)	

a) And own estimations: stack replacement after 10 years.
b) And own estimations: stack replacement after maximum lifetime of the stacks.
c) And own estimations; product gas cleaning included.

Techno-economic parameters of renewable energy technologies

For onshore wind turbines, 59 different configurations are taken into account for the year 2050. The hub heights vary between 80 and 160 m. The specific area output ranges between 270 and 500 W/m^2. A wind turbine with a hub height of 110 m and a specific area output of 400 W_{el}/m^2 costs 1160 €/kW_{el} in 2020 and 1050 €/kW_{el} in 2050. The costs are based on Wallasch, Lüers, Heyken, Rehfeldt, and Jachmann (2019).

(See Table A7 and A8)

Table A7
Hub height, rotor diameter, and specific investments for the considered offshore wind turbines in 2030 and 2050 (Koepp et al., 2019).

Turbine	Hub height (m)	Rotor diameter (m)	Specific investment (€/kW_{el})	
			2030	2050
1	100	400	3580	3422
2	100	450	3497	3341
3	110	400	3640	3482
4	120	350	3783	3622
5	120	360	3766	3607
6	120	380	3732	3574
7	120	400	3700	3542

Table A8
Specific investments for different solar technologies in 2030 and 2050; the costs are based on solar power plants from 2020 (Zentrum für Sonnenenergie- und Wasserstoff-Forschung Baden-Württemberg, 2019) and a learning rate (Fraunhofer ISE, 2015).

	Specific investment (€/kW_{el})	
Technology	2030	2050
Ground-mounted PV	662	500
Roof-top PV	933	765
CSP	2047	1442

References

Adolf, J., Fischedick, M., Balzer, C. H., Arnold, K., Pastowski, A., Louis, J., … Schüwer, D. (2017). *Shell Hydrogen Study: Energy of the future? Sustainable Mobility through Fuel Cells and H2*. Hamburg: Retrieved from. https://www.shell.de/medien/shell-publikationen/shell-hydrogen-study/_jcr_content/par/toptasks_e705.stream/1497968967778/1c581c203c88bea74d07c3e3855cf8a4f90d587e/shell-hydrogen-study.pdf.

Agora Verkehrswende, Agora Energiewende, & Frontier Economics (2018). The Future Cost of Electricity-Based Synthetic Fuels.

Atkinson, S. (2005). World's largest desalination plant begins operating in Israel. *Membrane Technology, 2005*(12), 9–10. https://doi.org/10.1016/S0958-2118(05)70589-9

Beltaifa, H. (2020). MENA - Electricity Transmission Network. Retrieved from https://energydata.info/dataset/mena-electricity-transmission-network-2017.

Bernath, C., Deac, G., & Sensfuß, F. (2019). Influence of heat pumps on renewable electricity integration: Germany in a European context. *Energy Strategy Reviews, 26*, 100389. https://doi.org/10.1016/j.esr.2019.100389

Bosch, J., Staffell, I., & Hawkes, A. D. (2017). Temporally-explicit and spatially-resolved global onshore wind energy potentials. *Energy, 131*, 207–217. https://doi.org/10.1016/j.energy.2017.05.052

Chardonnet, C., Vos, L. de, Genoese, F., Roig, G., Bart, F., Lacroix, T. de, . . . van Genabet, B. (2017). EARLY BUSINESS CASES FOR H2 IN ENERGY STORAGE AND MORE BROADLY POWER TO H2APPLICATIONS: FINAL REPORT.

Collins, L. (2019). World's first liquefied hydrogen carrier launched in Japan: The Suiso Frontier is a key part of the HySTRA demonstration project, which will see hydrogen shipped 9,000 km from southeast Australia to the Japanese city of Kobe: NHST Global Publications AS. Retrieved from https://www.rechargenews.com/transition/worlds-first-liquefied-hydrogen-carrier-launched-in-japan/2-1-722155.

Copernicus Climate Change Service (2020, July 15). ERA5: Fifth generation of ECMWF atmospheric reanalyses of the global climate: Copernicus Climate Change Service Climate Data Store. Date of access: May 2019. Retrieved from https://cds.climate.copernicus.eu/cdsapp.

Council of the European Union. (2009). *Presidency Conclusions 29–30 October 2009*. Brussels: Retrieved from. https://ec.europa.eu/regional_policy/sources/cooperate/baltic/pdf/council_concl_30102009.pdf.

D'Amore-Domenech, R., & Leo, T. J. (2019). Sustainable Hydrogen Production from Offshore Marine Renewable Farms: Techno-Energetic Insight on Seawater Electrolysis Technologies. *ACS Sustainable Chemistry & Engineering, 7*(9), 8006–8022. https://doi.org/10.1021/acssuschemeng.8b06779

Danielson, J. J., & Gesch, D. B. (2011). Global multi-resolution terrain elevation data 2010 (GMTED2010). Open-File Report. Advance online publication. https://doi.org/10.3133/ofr20111073.

Drechsler, C., & Agar, D. W. (2021). Characteristics of DAC operation within integrated PtG concepts. *International Journal of Greenhouse Gas Control, 105*, 103230. https://doi.org/10.1016/j.ijggc.2020.103230

Eurek, K., Sullivan, P., Gleason, M., Hettinger, D., Heimiller, D., & Lopez, A. (2017). An improved global wind resource estimate for integrated assessment models. *Energy Economics, 64*, 552–567. https://doi.org/10.1016/j.eneco.2016.11.015

European Commission (2018a). COMMUNICATION FROM THE COMMISSION TO THE EUROPEAN PARLIAMENT, THE EUROPEAN COUNCIL, THE COUNCIL, THE EUROPEAN ECONOMIC AND SOCIAL COMMITTEE, THE COMMITTEE OF THE REGIONS AND THE EUROPEAN INVESTMENT BANK COM(2018) 773: A Clean Planet for all A European strategic long-term vision for a prosperous, modern, competitive and climate neutral economy. Retrieved from https://eur-lex.europa.eu/legal-content/EN/TXT/?uri=CELEX:52018DC0773.

European Commission (2018b). In-depth analysis in support of the commission communication COM(2018) 773: A clean Planet for all - A European long-term strategic vision for a prosperous, modern, competitive and cimate neutral economy. Supplementary information.

Commission, E. (2019). *December 11)*. Brussels: The European Green Deal.

European Commission (2020, July 8). A hydrogen strategy for a climate-neutral Europe: Communication from the Commission to the European Parliament, the Council, the European Economic and Social Committee and the Committee of the Regions. Brussels.

European Space Agency and Université Catholique de Louvain. (2010). GlobCover 2009. Retrieved from http://due.esrin.esa.int/page_globcover.php.

Fasihi, M., Efimova, O., & Breyer, C. (2019). Techno-economic assessment of CO2 direct air capture plants. *Journal of Cleaner Production, 224*, 957–980. https://doi.org/10.1016/j.jclepro.2019.03.086

Fasold, H.-G. (2010). Langfristige Gasbeschaffung für Europa - Pipelineprojekte und LNG-Ketten. *Gwf-Gas| Erdgas, 528*.

Feng, J., Feng, L., Wang, J., & King, C. W. (2020). Evaluation of the onshore wind energy potential in mainland China—Based on GIS modeling and EROI analysis. *Resources, Conservation and Recycling, 152*, 104484. https://doi.org/10.1016/j.resconrec.2019.104484

Frank, E., Gorre, J., Ruoss, F., & Friedl, M. J. (2018). Calculation and analysis of efficiencies and annual performances of Power-to-Gas systems. *Applied Energy, 218*, 217–231. https://doi.org/10.1016/j.apenergy.2018.02.105

Franke, K., Sensfuß, F., Deac, G., Kleinschmitt, C., & Ragwitz, M. (2021). Factors affecting the calculation of wind power potentials: A case study of China. *Renewable and Sustainable Energy Reviews, 149*, 111351. https://doi.org/10.1016/j.rser.2021.111351

Fraunhofer, I. E. E. (2021). PtX-Atlas. Retrieved from https://maps.iee.fraunhofer.de/ptx-atlas/.

Fraunhofer Institute for Systems and Innovation Research. (2019). Enertile. Retrieved from https://www.enertile.eu/enertile-en/index.php.

Fraunhofer ISE (2015). Current and Future Cost of Photovoltaics. Long-term Scenarios for Market Development, System Prices and LCOE of Utility-Scale PV Systems: Study on behalf of Agora Energiewende. Retrieved from https://www.agora-energiewende.de/fileadmin/Projekte/2014/Kosten-Photovoltaik-2050/AgoraEnergiewende_Current_and_Future_Cost_of_PV_Feb2015_web.pdf.

Godron, P., Neubarth, J., Soyah, M., Asceri, V., Callegari, G., Cova, B., . . . Youssef, A. (2014). Desert power: Getting connected: Starting the debate for the grid infrastructure for a sustainable power supply in EUMENA.

Golling, C., Heuke, R., Seidl, H., & Uhlig, J. (2019). Roadmap Power to Gas.

Götz, M., Lefebvre, J., Mörs, F., McDaniel Koch, A., Graf, F., Bajohr, S., … Kolb, T. (2016). Renewable Power-to-Gas: A technological and economic review. *Renewable Energy, 85*, 1371–1390. https://doi.org/10.1016/j.renene.2015.07.066

Graves, C., Ebbesen, S. D., Mogensen, M., & Lackner, K. S. (2011). Sustainable hydrocarbon fuels by recycling CO2 and H2O with renewable or nuclear energy. *Renewable and Sustainable Energy Reviews, 15*(1), 1–23.

Gupta, N. (2016). A review on the inclusion of wind generation in power system studies. *Renewable and Sustainable Energy Reviews, 59*, 530–543. https://doi.org/10.1016/j.rser.2016.01.009

Hafez, A., & El-Manharawy, S. (2002). Economics of seawater RO desalination in the Red Sea region, Egypt.

Hamed, Y., Hadji, R., Redhaounia, B., Zighmi, K., Bâali, F., & El Gayar, A. (2018). Climate impact on surface and groundwater in North Africa: A global synthesis of findings and recommendations. *Euro-Mediterranean Journal for Environmental Integration, 3*(1), 1163. https://doi.org/10.1007/s41207-018-0067-8

Hank, C., Sternberg, A., Köppel, N., Holst, M., Smolinka, T., Schaadt, A., . . . Henning, H.–M. (2020a). Energy efficiency and economic assessment of imported energy carriers based on renewable electricity. Retrieved from 10.1039/d0se00067a.

Hank, C., Sternberg, A., Köppel, N., Holst, M., Smolinka, T., Schaadt, A., . . . Henning, H.–M. (2020b). Supplementary Information: Energy efficiency and economic assessment of imported energy carriers based on renewable electricity.

He, G., & Kammen, D. M. (2014). Where, when and how much wind is available? A provincial-scale wind resource assessment for China. *Energy Policy, 74*, 116–122. https://doi.org/10.1016/j.enpol.2014.07.003

Homann, K., Reimert, R., & Klocke, B. (2013). The Gas Engineer's Dictionary: Supply Infrastructure from A to Z: DIV.

Hoogwijk, M., de Vries, B., & Turkenburg, W. (2004). Assessment of the global and regional geographical, technical and economic potential of onshore wind energy. *Energy Economics, 26*(5), 889–919. https://doi.org/10.1016/j.eneco.2004.04.016

Hu, J., Harmsen, R., Crijns-Graus, W., & Worrell, E. (2019). Geographical optimization of variable renewable energy capacity in China using modern portfolio theory. *Applied Energy, 253*, 113614. https://doi.org/10.1016/j.apenergy.2019.113614

Hydrogen Council (2020). Path to hydrogen competitiveness: A cost perspective.

IEA (2020). Electricity Consumption by IEA Data Services. Retrieved from https://www.iea.org/subscribe-to-data-services/world-energy-balances-and-statistics.

International Energy Agency (2019). The Future of Hydrogen: Seizing today's opportunities.

International Energy Agency. (2020). World Energy Outlook 2020. . https://doi.org/10.1787/20725302

Deymann, J. (2014). Unkonventionelles Erdgas: Auswirkungen auf den globalen Erdgasmarkt.

Koepp, M., Krampe, L., Wendring, P., Eckstein, J., Richter, M., Schäfer-Frey, J., . . . Wilms, J. (2019). Vorbereitung und Begleitung bei der Erstellung eines Erfahrungsberichts gemäß §97 Erneuerbare-Energien-Gesetz: Teilvorhaben IIf: Windenergie auf See.

Leiblein, J., Bär, K., Graf, F., Kühn, M., Müller, S., Bäuerle, M., & Benthin, J. (2020). Roadmap Gas 2050 Deliverable D1.1: Bewertung von alternativen Verfahren zur Bereitstellung von grünem und blauem H2: DVGW-Förderkennzeichen G 201824.

Liu, C., Wang, Y., & Zhu, R. (2017). Assessment of the economic potential of China's onshore wind electricity. *Resources, Conservation and Recycling, 121*, 33–39. https://doi.org/10.1016/j.resconrec.2016.10.001

Lux, B., & Pfluger, B. (2020). A supply curve of electricity-based hydrogen in a decarbonized European energy system in 2050. *Applied Energy, 269*, 115011. https://doi.org/10.1016/j.apenergy.2020.115011

Mörs, F., Schlautmann, R., Gorre, J., & Leonhard, R. (2020). Innovative large-scale energy storage technologies and power-to-gas concepts after optimisation (STORE&GO): D 5.9 Final report on evaluation of technologies and processes. Retrieved from https://cordis.europa.eu/project/id/691797/results.

Niermann, M., Timmerberg, S., Drünert, S., & Kaltschmitt, M. (2021). Liquid Organic Hydrogen Carriers and alternatives for international transport of renewable hydrogen. *Renewable and Sustainable Energy Reviews, 135*, 110171. https://doi.org/10.1016/j.rser.2020.110171

Pfluger, B. (2014). *Assessment of least-cost pathways for decarbonising Europe's power supply: A model-based long-term scenario analysis accounting for the characteristics of renewable energies*. Karlsruhe: KIT Scientific Publishing.

Pfluger, B., Tersteegen, B., Franke, B., Bernath, C., Bossmann, T., Deac, G., … Reiter, U. (2017). *Langfristszenarien für die Transformation des Energiesystems in Deutschland. Modul 2: Modelle und Modellverbund*.

Rönsch, S., Schneider, J., Matthischke, S., Schlüter, M., Götz, M., Lefebvre, J., … Bajohr, S. (2016). Review on methanation - From fundamentals to current projects. *Fuel, 166*, 276–296. https://doi.org/10.1016/j.fuel.2015.10.111

Schäffer, J., Ortloff, F., Lubenau, U., Imberg, C., & Senner, J. (2019). Bewertung von Quellen und Abtrennungsverfahren zur Bereitstellung von CO2 für PtG-Prozesse: Abschlussbericht G201621, G 1/04/16.

Schildauer, T. J., & Biollaz, S. M. A. (2016). Synthetic Natural Gas from Coal, Dry Biomass, and Power-to-Gas Applications. Hoboken, New Jersey: John Wiley & Sons Inc. https://doi.org/10.1002/9781119191339.

Schlautmann, R., Böhm, H., Zauner, A., Mörs, F., Tichler, R., Graf, F., & Kolb, T. (2021). Renewable Power-to-Gas: A Technical and Economic Evaluation of Three Demo Sites Within the STORE&GO Project. *Chemie Ingenieur Technik, 9*(7), 50. https://doi.org/10.1002/cite.202000187

Schubert, G. (2012). Modeling hourly electricity generation from PV and wind plants in Europe. In I. Staff (Ed.), 2012 9th International Conference on the European Energy Market (pp. 1–7). [Place of publication not identified]: IEEE. https://doi.org/10.1109/EEM.2012.6254782.

Sebestyén, T.-T. (2017). Assessment of Solar PV Power Generation Potential in Centre Development Region of. *Romania, 5*(4), 299–303.

Siegemund, S., Trommler, M., Kolb, O., Zinnecker, V., Schmidt, P., Weindorf, W., . . . Zerhusen, J. (2019). The potential of electricity-based fuels for low-emission transport in the EU: E-Fuels study. Berlin.

Göß, S. (2017). Tutorial Gasmarkt Teil 6: Erdgastransport und -speicherung. Retrieved from https://blog.energybrainpool.com/tutorial-gasmarkt-teil_6-erdgastransport-und-speicherung/.

Smolinka, T., Wiebe, N., Sterchele, P., Palzer, A., Lehner, F., Jansen, M., . . . Zimmermann, F. (2018). Study IndWEDe: Industrialisation of water electrolysis in Germany: Opportunities and challenges for sustainable hydrogen for transport, electricity and heat. Berlin.

Songhurst, B. (2018). LNG plant cost reduction 2014-18: Oxford Institute for Energy Studies. https://doi.org/10.26889/9781784671204.

Stolzenburg, K., Berstad, D., Decker, L., Elliott, A., Haberstroh, C., Hatto, C., . . . Walnum, H. T. (2013). Efficient Liquefaction of Hydrogen: Results of the IDEALHY Project. XXth Energie-Symposium Stralsund.

Timmerberg, S. [Sebastian], & Kaltschmitt, M. [Martin] (2019). Hydrogen from renewables: Supply from North Africa to Central Europe as blend in existing pipelines – Potentials and costs. Applied Energy, 237, 795–809. https://doi.org/10.1016/j.apenergy.2019.01.030.

Timmerberg, Sebastian, Sanna, Anas, Kaltschmitt, Martin, & Finkbeiner, Matthias (2019). Renewable electricity targets in selected MENA countries – Assessment of available resources, generation costs and GHG emissions. *Energy Reports, 5*, 1470–1487. https://doi.org/10.1016/j.egyr.2019.10.003

Töpler, Johannes, & Lehmann, Jochen (Eds.). (2016). *Hydrogen and Fuel Cell*. Berlin, Heidelberg: Springer Berlin Heidelberg.

Ueckerdt, F., Bauer, C., Dirnaichner, A., Everall, J., Sacchi, R., & Luderer, G. (2021). Potential and risks of hydrogen-based e-fuels in climate change mitigation. *Nature Climate Change, 11*(5), 384–393. https://doi.org/10.1038/s41558-021-01032-7

United Nations (2015). Paris Agreement. Retrieved from https://unfccc.int/files/meetings/paris_nov_2015/application/pdf/paris_agreement_english_.pdf.

United Nations, Department of Economic and Social Affairs, Population Division (2019). World Population Prospects 2019: Online Edition. Rev. 1. Retrieved from https://population.un.org/wpp/Download/Standard/Population/.

Ursua, A., Gandia, L. M., & Sanchis, P. (2012). Hydrogen Production From Water Electrolysis: Current Status and Future Trends. *Proceedings of the IEEE, 100*(2), 410–426. https://doi.org/10.1109/JPROC.2011.2156750

Viebahn, P., Scholz, A., & Zelt, O. (2019). The Potential Role of Direct Air Capture in the German Energy Research Program-Results of a Multi-Dimensional Analysis. *Energies, 12*(18), 3443. https://doi.org/10.3390/en12183443

Wallasch, A.–K., Lüers, S., Heyken, M., Rehfeldt, K., & Jachmann, H. (2019). Vorbereitung und Begleitung bei der Erstellung eines Erfahrungsberichts gemäß §97 Erneuerbare-Energien-Gesetz: Teilvorhaben IIe): Wind an Land.

Wang, A., van der Leun, K., Peters, D., & Buseman, M. (2020). European Hydrogen Backbone: HOW A DEDICATED HYDROGEN INFRASTRUCTURE CAN BE CREATED.

Corporation, Wärtsilä (2016). LNG Plants Mini-scale Liquefaction Technology. Retrieved from https://www.wartsila.com/marine/build/gas-solutions/liquefaction-bog-reliquefaction/lng-plants-mini-scale-liquefaction-technology.

World Conservation Monitoring Centre. (2014). World Database on Protected Areas (WDPA). Retrieved from http://www.protectedplanet.net/.

WorldPop (2018). Global 1km Population. https://doi.org/10.5258/SOTON/WP00647.

Zauner, A., Böhm, H., Rosenfeld, D. C., & Tichler, R. (2019). Innovative large-scale energy storage technologies and Power-to-Gas concepts after optimization: D 7.7 Analysis on future technology options and on techno-economic optimization.

Zeman, F. S., & Keith, D. W. (2008). Carbon neutral hydrocarbons. *Philosophical Transactions. Series A, Mathematical, Physical, and Engineering Sciences, 366*(1882), 3901–3918. https://doi.org/10.1098/rsta.2008.0143

Zentrum für Sonnenenergie- und Wasserstoff-Forschung Baden-Württemberg (März 2019). Vorbereitung und Begleitung bei der Erstellung eines Erfahrungsberichts gemäß § 97 Erneuerbare-Energien-Gesetz: Teilvorhaben II c: Solare Strahlungsenergie. Erstellt im Auftrag des Bundesministeriums für Wirtschaft und Energie.

Zhou, Y., & Tol, R. S. J. (2005). Evaluating the costs of desalination and water transport. *Water Resources Research, 41*(3), 18. https://doi.org/10.1029/2004WR003749